GAS CHEMISTRY OF THE AHUACHAPÁN AND BERLÍN GEOTHERMAL FIELDS, EL SALVADOR

Patricia E. Jacobo
LaGeo S.A. de C.V.
15 Avenida Sur, Colonia Utila
Nueva San Salvador, La Libertad
EL SALVADOR, C.A.
pjacobo@lageo.com.sv

ABSTRACT

Gas compositions of reactive gases in geothermal fluids of the Ahuachapán and Berlín fields have been used to estimate sub-surface conditions such as temperature and initial aquifer steam fraction. Inert or conservative gas compositions provide information on the source of the gases in the reservoir liquid. Of the fourteen gas geothermometers used in this study, the H_2S and CO_2 geothermometers yield the best temperature values. The initial steam fractions in the aquifers of both Ahuachapán and Berlín geothermal reservoirs are low and generally negative, i.e. the aquifer water flowing into these wells has lost some steam. The computed concentrations of N_2 and Ar also indicate the presence of a secondary steam component in the well discharges.

1. INTRODUCTION

Presently, two geothermal fields are exploited in El Salvador, Ahuachapán and Berlín fields with installed capacity of 92 MWe and 56 MWe, respectively. During 2002, the Ahuachapán and Berlín fields produced 23% of the total electricity generation in the country.

El Salvador, along with the rest of Central America is a seismologically active region, situated atop three of the large tectonic plates that constitute the Earth's surface. The motion of these plates causes the area's earthquake and volcanic activity (Figure 1). The geodynamics of the region is mainly controlled by the subduction process of the Cocos plate under the Caribbean plate, which has created the deep Middle America Trench lying off the coast of El Salvador. Parallel to this trench runs the Central American graben, a structural depression 20 km wide that crosses the whole country, with flanks defined by normal W-E trending faults. On the southern margin of the graben, a Quaternary volcanic chain with heights of 1,500 to 2,000 m constitutes the heat source that produces widespread geothermal activity.

The present study involves the assessment of the gas chemistry of both the Ahuachapán and Berlín production fields. Interpretation of gas composition has been used to estimate reservoir conditions such as boiling, aquifer temperature and initial steam fraction. As these models are constrained by several assumptions, data interpretation has been based on assessment of the validity of the assumptions made.

2. THE AHUACHAPÁN GEOTHERMAL SYSTEM

2.1 Geological features

The Ahuachapán geothermal field is located by the southern flank of the central Salvadoran graben, and the northwest sector of the Cerro Laguna Verde volcanic group. This group constitutes a complex extrusive structure developed during Quaternary times near the Pliocene tectonic block of Tacuba-Apaneca. The geothermal reservoir of the Ahuachapán geothermal system seems to be genetically related to the regional tectonic evolution of the area. Permeable faults and fractures of this zone form the pathways for deep circulation of the parent meteoric water to the geothermal fluid. Where geothermal fluids reach the surface, acid surface alteration is seen with fumarolic zones, distributed around an area of 50 km^2 (Montalvo, 1994).

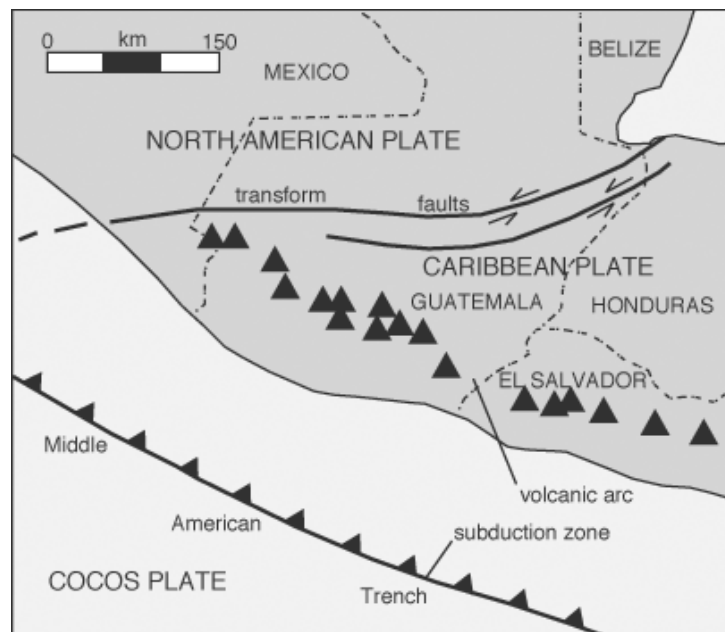The regional and local structures are controlled by a system of faults and

FIGURE 1: Simplified tectonic map of El Salvador and neighbouring region; subduction of the Cocos Plate beneath the Caribbean Plate produces the Central American arc; the arc is defined by the line of volcanoes (black triangles) (modified from Duffield et al., 1989)

fractures oriented along three main directions, E-W, which is approximately the trend of the main graben, a system of faults that strike NE-SW which is the most recent system of faults, and finally fractures that have a NNW-SSE trend.

The stratigraphic sequence of the Ahuachapán area is mainly formed by:

1. Tuff and lava formations (extrusive material) in the upper part of the system, with a thickness around 200 m;
2. Young agglomerate formation that is essentially impermeable, due to a high hydrothermal alteration that forms the cap rock of the reservoir with a thickness of up to 400 m;
3. Andesites of Ahuachapán, with a thickness of up to 300 m that form the productive geothermal reservoir which typically has secondary permeability; and
4. The older agglomerates in the lower part of the system that form the basement with a thickness in excess of 400 m (Montalvo, 1994).

2.2 Heat source

The heat source to the geothermal system is a recent andesite-basalt magmatic chamber, less than 0.1 My old, and located at 9 km depth. This source feeds the volcanic complex Laguna Las Ninfas, Hoyo de Cuajuste and Laguna Verde, which is located 3 km southeast of the geothermal field (CEL, 1997).

2.3 Alteration mineralogy

Table 1 summarizes the different zones or facies identified according to the mineralogical alteration.

TABLE 1:   Representative minerals in the production zone of the Ahuachapán geothermal field

Facies	Mineral composition	%	Formation temperature
Phyllic prophylithic 900-1500 m	Epidote – $Ca_2(Al,Fe)Al_2O(SiO_4)(Si_2O_7)(OH)$	Tz-1 (10-40, AH-33B)	210-230°C (250°C)
	Calcite – $CaCO_3$	2-32	
	Chlorite –$(Mg,Fe)_5(Si,Al)_5O_{10}(OH)_8$	1-15	
	Hematite – Fe_2O_3	1-10	
	Quartz – SiO_2	10-50	
	Anhydrite – $CaSO_4$	3-7 (18)	
	Wairakite – $CaAl_2Si_4O_{12}.2H_2O$	1-7	

2.4   The Ahuachapán production field

Power generation in the Ahuachapán geothermal field started in 1975. A total of 40 wells have been drilled (590-1524 m deep) in an area of approximately 5 km². In order to optimize the management of the field, at present only 8 wells are in continuous operation: AH-4bis, AH-6, AH-17, AH-20, AH-22, AH-23, AH-26 and AH-27 (Figure 2). The temperature in the reservoir of the Ahuachapán field is in the range 210-220°C, and the average reservoir pressure is approximately 20 bar-a, compared to 37 bar-a initially. Almost all the wells are operated at a separation pressure of 6-7 bar-a. (Montalvo, 1994). Reinjection of part of the separated water was carried out during 1975 – 1982 but stopped due to rise in wellhead injector pressures and cooling effects (Quijano, 1994). A new reinjection project was started in 2000 in the near Chipilapa field.
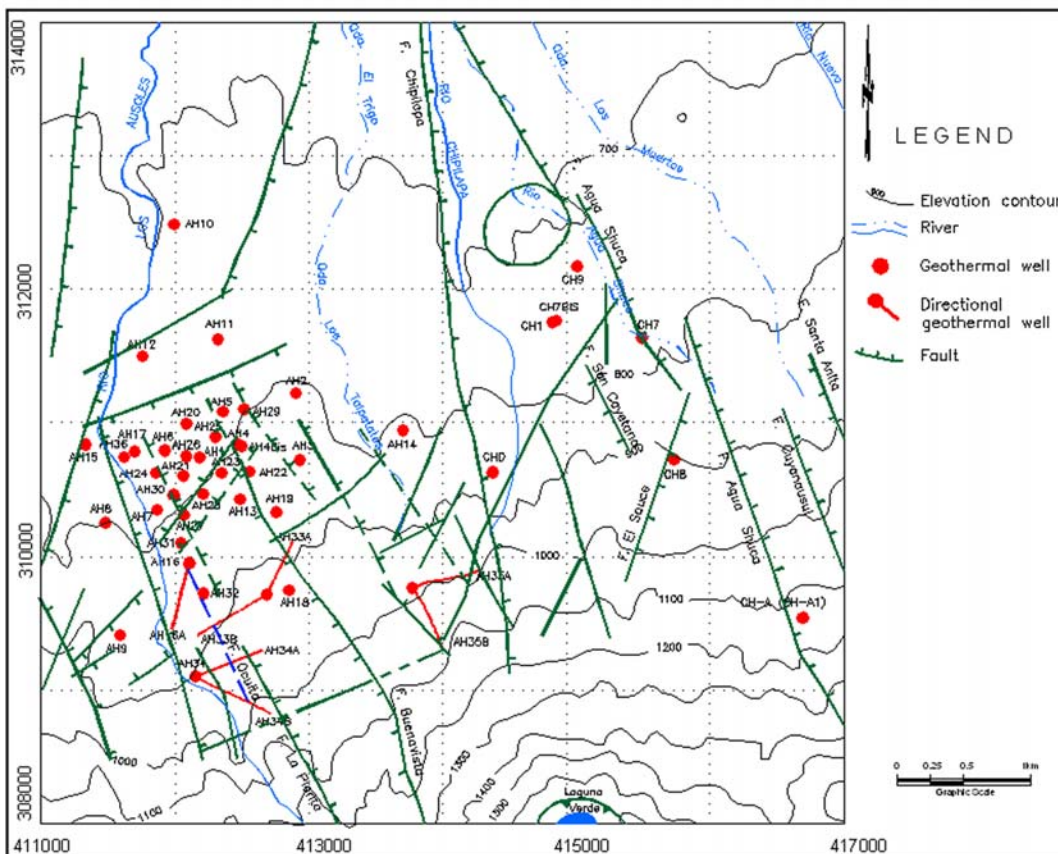

FIGURE 2:   The Ahuachapán geothermal system and the Ahuachapán production field

2.5 Fluid chemistry

The fluid extracted from the field is a two-phase mixture of steam and water, which is conducted to wellhead separators to obtain medium-pressure steam that directly feeds the three units of the power plant. With exploitation, several changes have occurred in the water and gas chemistry in the Ahuachapán field. In some wells in the north, discharge enthalpies increased strongly, consistent with the formation of a steam cap on the top of the reservoir. This happened in relatively shallow wells where the pressure in the local reservoir decreased considerably. The quartz temperature decreased strongly for the wells in the northern portion down to 200-218°C; while for the other wells the decline is less, with temperatures in the 225-235°C range. The reservoir chloride content shows a general decline in all wells down to about 6000 mg/kg. The cation geothermometers show, for almost all the wells, higher values than measured temperature values, ranging from 240 to 265°C (almost constant with respect to the initial values). This is due to an almost constant value of the Na/K ratio, which is not affected by the dilution shown by the chloride content. In the computed composition of the reservoir water, pH decreased from an original value of about 6 to a 1997 value of about 5, SO_4 content has increased, despite the decrease in chloride (D'Amore and Mejía, 1999).

Computed CO_2 partial pressure range from 0.03 to 0.3 Map; similar numbers for H_2S and H_2 are 0.0008-0.0028 and 0.0023-0.006 Map, respectively (D'Amore and Mejía, 1999).

3. THE BERLÍN GEOTHERMAL SYSTEM

3.1 Geological features

The Berlín geothermal field is located on the northern slope of the Berlín-Tecapa volcanic complex, which belongs to the Quaternary volcanic chain on the southern block of the Central America graben. The Berlín-Tecapa volcanic complex is formed by the Caldera of Berlín, strato volcanoes and cineritic cones. The Quaternary volcanoes are mainly built up of andesite lavas interlayered with andesitic, pyroclastics, and basalt lavas. The cineritic formations are mostly composed of scorias and basaltic-andesite ashes (GESAL, 2000).

A NW-SE fault system in the northern part of the Caldera of Berlín is considered the most important geothermally, because it permits the ascent of fluids from depth to the surface. The majority of the hydrothermal manifestations and the geothermal field itself are found inside this structure (Renderos, 2002) (see Figure 3).

3.2 Heat source

The heat source to the Berlín hydrothermal system is a recent degassing andesite magma chamber at a depth of around 6 km. The Berlín and Blanca Rosa Calderas were both formed through a process of magma chamber differentiation more than 100 and 75 thousand years ago, respectively. The flows of gray ignimbrite and white rose pumice are evident in the area. The later products of the Berlín-Tecapa strato volcano are less than 75 thousand years and are observed in the southern border of the Caldera Blanca Rosa and within the Caldera of Berlín. Other evidence of the magmatic or volcanic activity in this area is a phreatic eruption of El Hoyón crater, which was formed 700 years ago (GESAL, 2000).

3.3 Alteration mineralogy

The alteration mineralogy characterizing the Berlín geothermal field is due to the replacement of the original glass and minerals by secondary minerals. Table 2 summarizes the main hydrothermal mineral zones.
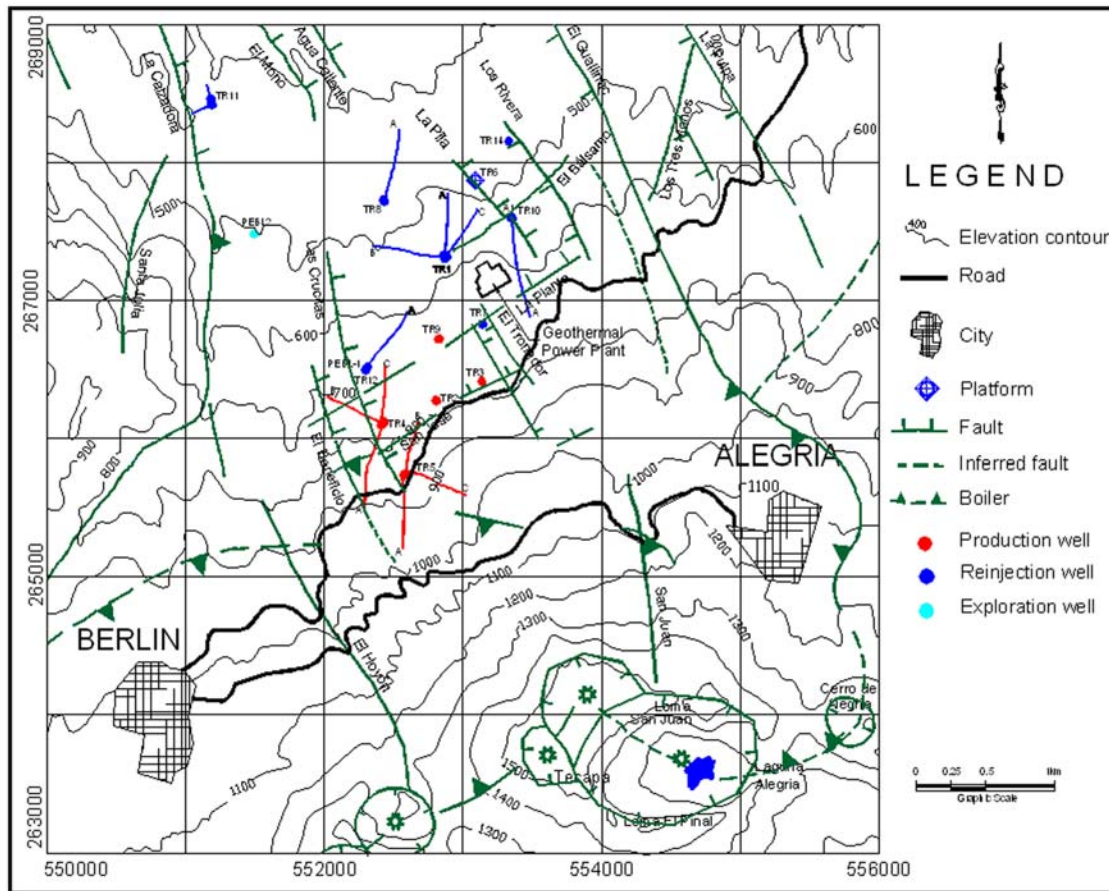
FIGURE 3: The Berlín geothermal system and the Berlín production field

TABLE 2: Representative minerals in the production zone of the Berlín geothermal field

Facies	Mineral composition	%	Formation temperature
Phyllic 1000-1500 m	Chlorite –$(Mg,Fe)_5(Si,Al)_5O_{10}(OH)_8$	(3) 10-50	200-220˚C
	Calcite – $CaCO_3$	7-20	
	Quartz – SiO_2	2-10	
	Epidote – $Ca_2(Al,Fe)Al_2O(SiO_4)(Si_2O_7)(OH)$	tz-2	
	Wairakite – $CaAl_2Si_4O_{12}.2H_2O$	1	
	Chlorite clay – $Mg_8Al_3Si_6O_{20}(OH)_{10}.4H_2O$	4	
Phyllic – prophylithic 1500-1800 m	Calcite – $CaCO_3$	20	220-250˚C
	Chlorite –$(Mg,Fe)_3(Si,Al)_4O_{10}(OH)_2(Mg,Fe)_3(OH)_6$	5-10	
	Sericitic/Ilithic - $K_{0.5}(Al, Fe, Mg)_3(Si,Al)_4O_{10}(OH)_2$	5-25	
	Epidote– $Ca_2(Al,Fe)Al_2O(SiO_4)(Si_2O_7)(OH)$	1-10	
	Quartz – SiO_2	3-15	
	Penine –$(Mg,Fe)_3(Si,Al)_4O_{10}(OH)_2(Mg,Fe)_3(OH)_6$	1	
	Wairakite– $CaAl_2Si_4O_{12}.2H_2O$	30	
	Prehnite – $Ca_2Al(AlSi_3O_{10})(OH)_2$	1-7	
	Pyrite – FeS	1	
Prophylithic 1800 - >2000 m	Chlorite –$(Mg,Fe)_3(Si,Al)_4O_{10}(OH)_2(Mg,Fe)_3(OH)_6$	5-9	250-300˚C
	Prehnite – $Ca_2Al(AlSi_3O_{10})(OH)_2$	5-7	
	Epidote– $Ca_2(Al,Fe)Al_2O(SiO_4)(Si_2O_7)(OH)$	5-30	
	Actinolite – $Ca_2(Mg,Fe)_5Si_8O_{22}(OH)_2$	1-7	
	Quartz – SiO_2	2-30	

3.4 The Berlín production field

The characteristics of the Berlín field are very different from that of Ahuachapán. The wells in the Berlín field range in depth from 1.5 to 2.4 km with temperatures close to 300°C in the southern production zone (wells TR2, TR4 and TR5). Measured temperatures decrease towards the north, where the measured values in wells TR1, TR8, TR10 and TR14 are of the order of 139°C (reinjection zone). In Berlín, reinjection has been adopted since the beginning of production in 1991, when two wellhead units were installed using wells TR-2 and TR-9 as producers and well TR-1 as reinjector (D'Amore and Mejía, 1999).

3.5 Fluid chemistry

The average temperature in the liquid-dominated geothermal field of Berlín is close to 300°C in the southern production zone, in wells TR-2, TR-4, and TR-5. The discharged fluids are classified as sodium-chloride type with chloride content of 3,000-7,000 ppm, pH values between 5 and 8 and salinity between 7,000 and 20,000 ppm. The gas/steam ratio is usually between 0.001 and 0.003 (Renderos, 2002). The isotopic composition of the water discharged from the wells shows evidence of the effect of reinjection. In the δ^2H-$\delta^{18}O$ diagram, the points of the producing wells are located between the isotopic composition of the local recharge meteoric water and the isotopic composition of the injected water (D'Amore and Mejía, 1999).

4. CHEMISTRY OF GEOTHERMAL GASES

4.1 Introduction

Gas composition of reactive gases in geothermal fluids has been widely used to estimate sub-surface conditions such as temperature and steam fraction beyond the depressurization zone. Furthermore, inert or conservative gas compositions can be used to provide information on the source of the gases in the geothermal fluid. The solubility of a gas in the liquid phase of a geothermal fluid governs the extent to which it fractionates into the vapour phase on steam formation. For the common geothermal gases, the solubility order is: $NH_3 > H_2S > CO_2 > CH_4 > H_2 > O_2 > N_2$ (Nicholson, 1993).

Gas concentrations of reservoir fluids which are controlled by mineral/solute equilibria increase with increasing equilibrium steam fraction, particularly for the less water-soluble gases. However, according to Arnórsson et al. (1990), steam fractions in the reservoir fluid of liquid-dominated geothermal systems, generally seem to be so low that they have relatively limited effect on the gas content of that fluid.

In a single-phase, hot-water reservoir, steam is formed as a consequence of pressure reduction as the fluid migrates to the surface. Under these circumstances, the steam chemistry, either at a fumarole or well discharge, is a direct consequence of the reservoir fluid composition. A more complex situation exists in two-phase reservoirs; these contain both vapour and liquid phases in equilibrium. In this case, the steam discharged at the surface will be a composite mixture of the reservoir vapour plus steam produced by boiling of the ascending liquid phase. Under these circumstances, the gas chemistry of the discharge may not reflect the gas-gas or gas-liquid equilibria present in the reservoir (Nicholson, 1993).

4.2 Gas content

The N_2/Ar ratio usually expected in geothermal fluids varies from 38 (for air-saturated water) to 84 (free air). The main indicator of air contamination is the presence of oxygen in the gas sample, combined with gas composition similar to Earth's atmosphere: $N_2/Ar = 84$ (Table 3); and $He/Ar = 5.7 \times 10^{-4}$ (Nicholson, 1993).

TABLE 3:   Concentration of gases in the atmosphere of Earth (Faure, 1991)

Component	%
CO_2	0.033
N_2	78.084
Ar	0.934
O_2	20.946

In air-saturated water, the theoretical content of N_2 and Ar at a given temperature can be estimated from the respective temperature equations for the solubility constant (K_s), (Table 4).

TABLE 4:   Temperature equations for the solubility constants (K_s) for gases
commonly found in geothermal fluids (Arnórsson and D'Amore, 2000)

Gas	Log K_s (T in Kelvin)
CO_2	- 59.612 + 3448.59 / T - 0.68640×10^{-6} T^2 + 18.847 log T
H_2S	- 68.775 + 3673.08 / T - 4.07153×10^{-6} T^2 + 22.56 log T
H_2	- 25.260 + 1355.28 / T - 4.11147×10^{-6} T^2 + 6.966 log T
N_2	- 55.857 + 2947.41 / T + 2.68428×10^{-6} T^2 + 17.191 log T
Ar	- 62.606 + 3136.06 / T - 1.00993×10^{-6} T^2 + 19.931 log T

At 25˚C:

$$K_s^{N_2} = N_2(mol/kg/bar) = 6.39 \times 10^{-4} = \frac{N_{2\,aq}}{N_{2\,gas}} \Rightarrow N_{2\,aq} = 6.39 \times 10^{-4} \frac{78.084}{100} = 4.99 \times 10^{-4} mol/kg/bar$$

$$N_{2\,aq} \text{ in air} - saturated \ water(mmol/kg_{H_2O}) = 4.99 \times 10^{-4}1000 = 0.5$$

$$K_s^{Ar} = Ar(mol/kg/bar) = 1.3822 \times 10^{-3} = \frac{Ar_{aq}}{Ar_{gas}} \Rightarrow Ar_{aq} = 1.3822 \times 10^{-3} \frac{0.934}{100} = 1.291 \times 10^{-5} mol/kg/bar$$

$$Ar_{aq} \text{ in air} - saturated \ water(mmol/kg_{H_2O}) = 1.291 \times 10^{-5}1000 = 0.013$$

4.3   Source of gases

Giggenbach (1991) combined the proportions of N_2, He, and Ar to produce a diagnostic ternary plot to aid identification of the dominant source of the gases. On the basis of a large number of analyses of gases discharged from a wide variety of terrestrial sources, data points in the plot were found to occupy an area delineated by three major source components:

a. *A meteoric component.* This component corresponds to air saturated groundwater. The N_2/Ar ratio is about 38 or somewhat higher, due to entrainment of air bubbles. The He/Ar ratio is lower than 0.001 (Giggenbach, 1991; Nicholson, 1993).
b. *A magmatic component.* The presence of a magmatic component increases considerably the N_2/Ar and He/Ar ratios compared to those of the meteoric component. Generally, N_2/Ar is about 800, but ratios of up to 2000 have been observed in andesitic gases associated with convergent plate boundaries, such as the Central American trench. The He/Ar ratio is about 0.1 (Giggenbach, 1991; Nicholson, 1993).
c. *A crustal component.* This component is made up largely of radiogenic He, therefore the He/Ar ratio is characteristically several orders of magnitude greater than the atmospheric value of 5.7 x 10^{-4}. Moreover, the helium-4 content is expected to increase with increasing residence time of the gases in the crust (Giggenbach, 1991; Nicholson, 1993).

4.4 Gas geothermometers

Studies in many high-temperature geothermal fields (> 200ºC) indicate that the concentrations (or ratios) of gases like CO_2, H_2S, H_2, N_2, NH_3, and CH_4 are controlled by temperature-dependent gas-gas and/or mineral-gas equilibria (D'Amore and Arnórsson, 2000). On this basis, data from chemical analyses of those gases have been used to develop relationships between the relative gas concentrations and the temperature of the reservoir. Such relationships are known as *gas or steam geothermometers*.

Gas geothermometers are also based on certain chemical reactions between gaseous species and minerals which are considered to be in chemical equilibrium. For each chemical equilibrium considered, a thermodynamic equilibrium constant may be expressed in terms of temperature, in which case the concentration of each gas species is often represented by its partial pressure in the vapour phase (D'Amore and Truesdell, 1985).

There are essentially three types of steam geothermometers. The first group is based on gas-gas equilibria. The second group is based on mineral-gas equilibria involving H_2S, H_2 and CH_4 but assuming CO_2 to be externally fixed. The third group is based on mineral-gas equilibria. The first two groups of geothermometers require only data on the relative abundance of gaseous components in a gas phase, whereas the third group calls for information on gas concentrations in steam (D'Amore and Arnórsson, 2000).

When using gas geothermometry, it is important to keep in mind that several factors other than aquifer temperature may affect the gas composition of a geothermal fluid. In geothermal reservoir fluids, gas concentrations at equilibrium depend on the ratio of steam to water of that fluid, whereas the gas content of fumarole steam is also affected by the boiling mechanism in the upflow, steam condensation and the separation pressure of the steam from the parent water. Furthermore, the flux of gaseous components into geothermal systems from their magmatic heat source may be quite significant and influence how closely gas-gas and mineral-gas equilibria are approached in specific aquifers (D'Amore and Arnórsson, 2000).

4.5 Initial aquifer steam fraction (Y)

The steam to water ratio in the aquifer under undisturbed or natural conditions is known as *initial aquifer steam fraction (Y)*. Basically, the term refers to the steam to water ratio of producing wells beyond the depressurization zone that forms as a result of mass withdrawal from the aquifer by the producing wells (Arnórsson and D'Amore, 2000).

Two geochemical methods have been used to estimate the initial aquifer steam fraction. They are based on different approaches. One assumes that the total discharge composition of wells is representative of the aquifer fluid. The other approach considers that both heat transfer from rock and phase segregation may contribute to the discharge enthalpy of the wells. If phase segregation occurs, the composition of the total well discharge will differ from that of the initial aquifer. The first model really assumes that excess enthalpy of well discharges is only caused by heat flow from the rock to the fluid flowing into the well (Arnórsson and D'Amore, 2000).

Model I
D'Amore (1998) has developed a method which is able to estimate both the aquifer temperature and the excess steam based on the Fischer-Tropsch reaction and a combined pyrite-magnetite and pyrite-hematite equilibria. The solution of equations produced a grid FT-HSH2 from which, in a graphical way, the reservoir temperature and the excess steam can be obtained (Barragán et al., 2000; Barragán et al., 2003).

The method *FT-HSH2* assumes the gas composition of total well discharges to be representative of the aquifer fluid and it is based on the following chemical equilibria:

$$CH_4 + H_2O = 4H_2 + CO_2$$
$$1.25H_2 + 1.5\,FeS_2 + 0.75\,Fe_2O_3 + 1.75H_2O = 3H_2S + Fe_3O_4$$
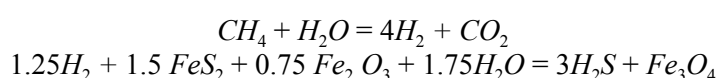
Several things should be considered when using model I (D'Amore and Mejía, 1999; Barragán et al., 2000):

- Thermodynamic equilibrium must be attained in the considered reactions;
- All the considered chemical species, including H_2O, must be in both chemical and phase equilibrium;
- No H_2O mass gain or loss is allowed after the original equilibrated system. Inflow of shallow recharge water will produce an underestimate of the computed temperature and Y values. A similar condition may be present when the reinjected water, or part of it, does not re-equilibrate with the gas in the reservoir;
- The fluid at the wellhead generally consists of a mixture of fluids coming from various volumes or sources of the reservoir with different chemical and physical characteristics. What we can obtain through the application of this method are integrated resultant values of the steam fraction Y and the temperature for all these different sources. This is especially important when the different sources have different gas/H_2O ratios. Exploitation can induce production from new regions of the reservoir having different fluid compositions. When a deep hot zone of the reservoir located below the exploited reservoir, rich in reactive species and CO_2, becomes an important fraction of the produced gas, an overestimation of the local reservoir temperature and Y values are obtained;
- An inflow of an external source of CO_2, not equilibrated with reservoir gases, can derive from the local accumulation of CO_2 at high pressure, because of condensation phenomena near the borders of the field. Its mixing with the fluid of the exploited low-pressure reservoir will cause an overestimate of the Y values;
- Differences or changes with time in the source temperature. Although this method allows us to calculate a slow change in temperature with time in a local part of the reservoir, it is unable to discriminate between different vertical parts having different temperatures and producing different fluids at the same time;
- It is assumed that there is no re-equilibration of the chemical species from the source or sources to wellhead.

Model II

Model II was developed by Arnórsson et al. (1990). This model evaluates boiling processes in the producing aquifers of "excess enthalpy" wet-steam wells using data on the concentration ratios of CO_2/H_2 or H_2S/H_2 in the discharged steam. The model permits calculation of: 1) the initial steam fraction; 2) the extent to which water and steam separate in the producing aquifer; and 3) the amount of enhanced evaporation due to heat flow from the rock to the boiling water. If phase segregation occurs in producing aquifers, the total well discharge composition is not the same as that of the initial aquifer fluid (Arnórsson and D'Amore, 2000).

In general, it is assumed that H_2S/H_2 ratios give more reliable estimates of Y than CO_2/H_2 ratios, largely because there is larger difference in solubility between H_2S and H_2 than there is between CO_2 and H_2. The reliability of the results obtained for the initial steam fraction depends on various factors including the selected values for the aquifer temperature; chemical reactions between gases and with minerals in the aquifer in the zone of depressurization; departure from equilibrium in the initial aquifer fluid; inaccuracy of the equations to describe gas solubilities; and inaccuracy in the equations used to describe the aqueous concentrations of CO_2, H_2S and H_2 in the undisturbed aquifer (Arnórsson and D'Amore, 2000).

In order to check the validity of each model, Arnórsson and D'Amore (2000) recommend for high-discharge enthalpy wells, to compare quartz, Na/K and Na/K/Ca geothermometry temperatures. If the quartz equilibrium temperature is similar to the Na/K and Na/K/Ca temperatures, it is likely that the assumption of Model I is valid, namely that the total discharge composition is representative of the initial aquifer fluid. Otherwise, if quartz equilibrium temperature, as calculated from the total discharge composition, is much lower than the Na/K temperature but similar if adiabatic boiling is assumed, it is considered likely that phase segregation is largely responsible for the elevated discharge enthalpy, in accordance with Model II.

5. METHODOLOGY

5.1 Sampling and analysis of geothermal gases

Most of the gas samples considered for the present study were collected at the wellhead using a stainless steel Webre mini separator at constant pressure. Some other samples were collected at the wellhead separator. The sampling technique consisted of using Giggenbach bottles containing 50 ml of 4M NaOH in order to retain the condensable gases, CO_2 and H_2S. All the non-condensable gases remained in the gas phase. Table 5 lists the analytical methods used for the analysis of the gas samples.

TABLE 5: Analytical methods used for gas analysis

Gas	Method
CO_2	Titration with HCl
H_2S	Titration with sodium tiocyanate
He	Gas chromatography with thermal conductivity detection
H_2	Gas chromatography with thermal conductivity detection
N_2	Gas chromatography with mass detection
Ar	Gas chromatography with mass detection
CH_4	Gas chromatography with mass detection
O_2	Gas chromatography with mass detection

5.2 Data handling

The study was carried out using samples collected in Ahuachapán and Berlín production fields during the year 2002. In the present report, the Ahuachapán wells are labelled AH and the Berlín wells as TR.

The composition of the fluid was estimated from the analytical data on the samples collected at the wellhead, based on two major assumptions. Firstly, the steam and water phases in the reservoir were assumed to be in phase equilibria. Secondly, samples at wellhead derive in large part from the vaporization of the liquid phase existing in the reservoir. On this basis, the fluid composition used in geothermometers and steam fraction equations was estimated from the relation:

$$m_i^t = m_i^{liq}\,(1-x) + m_i^{vap} x \tag{1}$$

where m_i^t = Concentration of component i in the discharge;
m^{liq} = Concentrations of the component i in the liquid; and
m^{vap} = Concentrations of the component i in the vapour phases, respectively;
x = Steam fraction in the discharge at the respective sampling pressure

The steam fraction in the discharge was estimated by the well known expression:

$$x = \frac{h^d - h^w}{L} \tag{2}$$

where h^d = Enthalpy of the discharge;
h^w = Enthalpy of liquid water at the temperature or pressure of separation and
L = Latent heat of vaporization at the same temperature.

For species not analysed in two phases, Equation 1 was simplified into the expressions:

$$m_i^t = m_i^{vap} x \tag{3}$$

$$m_i^t = m_i^{liq}(1-x) \tag{4}$$

When calculations required the use of concentrations at conditions different from those at sampling (e.g. 100°C or 1 bar) we have for conservation of mass:

$$m^{vap}_{i,\,condition\ 1}\, x_{condition\ 1} = m^{vap}_{i,\,condition\ 2}\, x_{condition\ 2} \tag{5}$$

$$m^{liq}_{i,\,condition\ 1}\,(1-x)_{condition\ 1} = m^{liq}_{i,\,condition\ 2}\,(1-x)_{condition\ 2} \tag{6}$$

where the letters m and x have the same meaning as above.

Estimation of the values for the different gas and water geothermometers was carried out by using the equations in Appendix I. The two models by D'Amore (1998) and Arnórsson et al. (1990), respectively, were applied to estimate the initial aquifer steam fraction:

Model I. The mass fraction of initial aquifer steam was estimated on the basis of the mole fraction of H_2 and H_2S in well discharges at a selected value for the aquifer temperature. Inserting the values in the right hand side of Equations 7 and 8, the analytical parameters *FT* and *HSH2* were obtained.

$$FT = 4\log\left(\frac{n_{H_2}}{n_{H_2O}}\right) + \log\left(\frac{n_{CO_2}}{n_{H_2O}}\right) - \log\left(\frac{n_{CH_4}}{n_{H_2O}}\right) \tag{7}$$

$$HSH2 = 3\log\left(\frac{n_{H_2S}}{n_{H_2O}}\right) - \tfrac{5}{4}\log\left(\frac{n_{H_2}}{n_{H_2O}}\right) \tag{8}$$

Model II. The mass fraction of initial aquifer steam obtained from the H_2 and H_2S content of the discharged steam (Y_{HS}) was calculated by the equation:

$$\%Y_{HS} = \frac{A_H - A_S}{\dfrac{55.51}{P}\left[\dfrac{A_S}{K_{H_2}} - \dfrac{A_H}{K_{H_2S}}\right] + (A_H - A_S)} \times 100 \tag{9}$$

where A_H $= m^v_{H2} / m^{f,\,l}_{H2}$;
  A_S $= m^v_{H2S} / m^{f,\,l}_{H2S}$;
  m^v_{H2} $= H_2$ moles/kg in steam sampled;
  $m^{f,\,l}_{H2}$ $= H_2$ moles/kg in aquifer water at the selected aquifer temperature estimated by using the equations in Table 6;
  m^v_{H2S} $= H_2S$ moles/kg in steam sampled;
  $m^{f,\,l}_{H2S}$ $= H_2S$ moles/kg in aquifer water at the selected aquifer temperature estimated by using the equations in Table 6;
  K_{H2S} $= H_2S$ solubility constant given in Table 4;
  K_{H2} $= H_2$ solubility constant given in Table 4.

In a similar way, the mass fraction of initial aquifer steam obtained from the H_2 and CO_2 content of the discharged steam (Y_{HC}) was calculated by the equation:

$$\%Y_{HC} = \frac{A_H - A_C}{\dfrac{55.51}{P}\left[\dfrac{A_C}{K_{H_2}} - \dfrac{A_H}{K_{CO_2}}\right] + (A_H - A_C)} \times 100 \tag{10}$$

where A_C $= m^v_{CO2} / m^{f,\,l}_{CO2}$;
  m^v_{CO2} $= CO_2$ mmoles/kg in steam sampled;
  $m^{f,\,l}_{CO2}$ $= CO_2$ mmoles/kg in aquifer water at the selected aquifer temperature estimated by using the equations in Table 6;
  K_{CO2} $= CO_2$ solubility constant given in Table 4.
  Other terms have the same meaning as above.

TABLE 6:   Temperature equations for the equilibrium constant for selected mineral-gas buffers;
they are valid in the range 0-350°C at vapour saturation pressures and assume unit activity
for all minerals, and liquid water (Karingithi, 2002)

Gas	Reaction	Log K (T)
CO_2	$CO_2 = czo + cal + \frac{3}{2} qtz + H_2O = \frac{3}{2} pre + CO_{2\,aq}$	$\log K(T) = -1.297 - 771.80/T + 0.007134\,T - 0.310\log T$
H_2S	$H_2S = \frac{1}{3} pyr + \frac{1}{3} pyrr + \frac{2}{3} pre + \frac{2}{3} H_2O = \frac{2}{3} epi + H_2S_{aq}$	$\log K(T) = -0.481 - 3129.34/T + 0.005705\,T + 0.187\log T$
H_2	$H_2 = \frac{4}{3} pyr + \frac{2}{3} pyrr + \frac{2}{3} H_2O = \frac{2}{3} epi + \frac{2}{3} pyr + H_{2\,aq}$	$\log K(T) = -2.411 - 1296.88/T + 0.006830*T - 0.725*\log T$

6. RESULTS

The primary chemical data for Ahuachapán and Berlín wells are given in Appendix II.

6.1 Gas content

The aquifer fluids from wells in the Ahuachapán and Berlín fields show relatively low total gas content.
The major components are CO_2 and H_2S (Table 7).

Ahuachapán
The total gas composition of the Ahuachapán field is shown in Table 7. According to these data,
individual gas concentrations of low-enthalpy wells such as AH-16A, AH-19, AH-20, AH-21, AH-22,
AH-28 range from 165 to 600 mg/kg. The rest of wells range from 692 to 1,714 mg/kg. Computed N_2
concentrations in the aquifer fluid range from 0.07 to 0.75 mmol/kg. Similar numbers for CO_2, H_2S, Ar
and H_2 are: 3.49-37.91; 0.27-1.21; 0.007-0.0076 and 0.0032-0.0697 mmol/kg, respectively.

Berlín
The individual total gas concentrations of the wells in the Berlín field range from 539 to 1,180 mg/kg
(Table 7). Computed N_2 concentrations in the aquifer fluid range from 0.16 to 0.48 mmoles/kg. Similar
numbers for CO_2, H_2S, Ar and H_2 are: 10.13-24.24, 1.93-2.90, 0.0017-0.0081, and 0.0229-0.1537
mmol/kg, respectively.

6.2 Source of gases and boiling

The calculated concentrations of N_2 and Ar in the aquifer fluid are lower than those for air saturated
water. This indicates that the reservoir water, which boils by depressurization in producing aquifers,
has been partially degassed, i.e. a component of secondary steam is present in the well discharges.
Primary steam formed during initial boiling is enriched in gas, partially in those gases which have low
solubility in water, such as N_2 and H_2.

The estimated N_2/Ar ratios are somewhat higher than in air-saturated water, which is taken to indicate
supply of N_2 to the well fluid other than the atmosphere. The high N_2/He ratio as well as the triangular
diagrams (Figure 4) suggest a component of andesitic magma origin.

TABLE 7:   Calculated gas concentrations (mmoles/kg) in the aquifer fluid of
the Ahuachapán and Berlín wells

Well	T_{ref} [a] (°C)	X_{aq} [b]	He	H_2	Ar	N_2	CH_4	CO_2	H_2S	N_2/Ar	He/Ar	mg/kg	% CO_2
AH-4BIS	230	0.25	2.59E-04	0.0292	0.0034	0.44	0.0082	22.74	0.47	130	0.077	1,029	96
AH-6	228	0.25	1.91E-04	0.0697	0.0028	0.42	0.0082	36.92	1.09	149	0.069	1,674	96
AH-16A	252	0.30	9.19E-05	0.0205	0.0018	0.22	0.0151	13.12	0.45	125	0.052	600	95
AH-17	244	0.28	1.51E-04	0.0174	0.0019	0.35	0.0042	31.18	1.21	180	0.079	1,423	95
AH-19	228	0.25	3.13E-05	0.0049	0.0009	0.09	0.0010	3.49	0.27	101	0.036	165	90
AH-20	231	0.26	3.05E-05	0.0092	0.0010	0.09	0.0012	7.64	0.27	92	0.031	348	95
AH-21	239	0.27	4.70E-05	0.0101	0.0011	0.13	0.0025	12.12	0.46	119	0.044	553	95
AH-22	229	0.25	8.67E-05	0.0148	0.0023	0.22	0.0029	10.91	0.36	95	0.038	499	95
AH-23	234	0.26	4.46E-04	0.0313	0.0076	0.75	0.0129	37.91	0.70	100	0.059	1,714	96
AH-26	228	0.25	1.79E-04	0.0386	0.0027	0.38	0.0078	31.15	0.75	140	0.066	1,407	96
AH-27	255	0.31	2.06E-04	0.0260	0.0028	0.38	0.0102	28.61	0.71	135	0.072	1,295	96
AH-28	250	0.30	1.60E-05	0.0032	0.0007	0.07	0.0005	5.54	0.33	96	0.023	257	93
AH-33B	241	0.28	1.62E-04	0.0184	0.0024	0.30	0.0035	16.79	0.63	127	0.068	769	95
AH-35A	221	0.24	4.68E-05	0.0062	0.0020	0.15	0.0014	15.12	0.65	79	0.024	692	95
TR-2	280	0.36	4.79E-05	0.0264	0.0031	0.21	0.0043	10.63	2.40	66	0.015	556	80
TR-4B	288	0.38	7.58E-05	0.1252	0.0081	0.48	0.0113	24.24	2.90	59	0.009	1,180	87
TR-4C	278	0.36	7.98E-05	0.1537	0.0070	0.39	0.0085	16.75	2.58	56	0.011	837	84
TR-5A	291	0.39	8.48E-05	0.0332	0.0023	0.31	0.0051	10.13	2.46	135	0.036	539	78
TR-5B	287	0.38	9.34E-05	0.0405	0.0034	0.28	0.0036	11.59	2.25	83	0.027	595	82
TR-5C	278	0.36	4.45E-05	0.0229	0.0017	0.17	0.0037	10.72	2.23	99	0.027	553	82
TR-5V	293	0.39	1.07E-04	0.0364	0.0041	0.32	0.0061	14.21	2.84	78	0.026	732	82
TR-9	273	0.35	2.92E-05	0.0309	0.0018	0.16	0.0030	10.72	1.93	88	0.017	542	83

[a] Average temperature estimated with quartz, Na/K and Na/K/Ca geothermometers (Table 8).
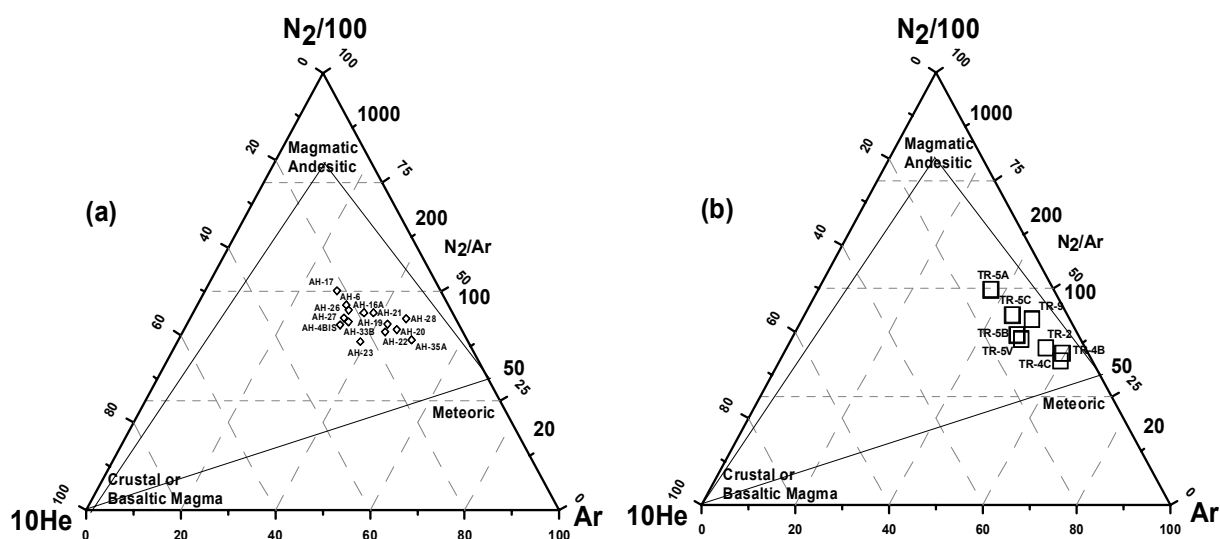[b] Steam fraction in the aquifer fluid assuming adiabatic boiling in one step to 1 bar (100°C).

FIGURE 4:   Source of gases in the geothermal fluid, (a) the Ahuachapán field; and (b) the Berlín field

6.3 Geothermometry

6.3.1 Gas geothermometers

Geothermometer temperatures have been calculated for eleven gas geothermometers shown in Table 8. Five of them have been empirically (geochemically) calibrated (Arnórsson and Gunnlaugsson, 1985) but the others have been calibrated using thermodynamic (theoretical) data (D'Amore and Panichi, 1980; Giggenbach, 1991; Nehring and D'Amore, 1984). Water temperatures have also been estimated using the quartz, Na/K and Na/K/Ca geothermometers. The gas and water geothermometer temperatures are given in Table 8, and the difference between each gas geothermometer and the average of the water temperatures is shown in Table 9.

D´Amore geothermometer
For the Ahuachapán field, this geothermometer yields temperature values ranging from 195 to 225˚C which are about 26 degree lower, on average, than the water temperatures. Similarly, in Berlín wells the geothermometer results are on average, 20 degree lower than the water temperature and range from 251 to 287˚C. This geothermometer, which is geochemically calibrated, uses H_2, H_2S and CH_4 concentrations in steam. They are considered to be controlled by equilibria but CO_2 is taken to be externally fixed.

CH_4/CO_2 geothermometer
Of the eleven gas geothermometers, the Fisher-Tropsch (FT) geothermometer indicates the highest temperatures. For the Ahuachapán field, this geothermometer yields temperature values ranging from 347 to 465˚C which are about 175 degree higher than the aquifer temperatures selected. In the Berlín wells, the geothermometer results range from 378 to 402˚C which are in average 105 degree higher than the water temperatures. These high temperatures, relative to other geothermometers and to measured temperatures, suggest that equilibrium for this reaction, which is very slow, has not been closely approached in the respective geothermal reservoirs.

H_2/Ar and CO_2/Ar geothermometers
These geothermometers are based on the ratio of a reactive gas (CO_2 or H_2) to the chemically inert argon. The calibration assumes that the Ar concentration in the aquifer fluid is that of air-saturated water (Giggenbach, 1991).

The H_2/Ar geothermometer in the Ahuachapán wells yields values from 211 to 272˚C, which are, on average, relatively close to the estimated aquifer temperatures. For the Berlín wells, the same geothermometer calculates values from 240 to 268˚C, which are on average 29˚C below the water temperatures. The CO_2/Ar geothermometer in Ahuachapán wells yields values from 265 to 293˚C, which are on average 43˚C above the water temperatures. The Berlín wells possess values from 254 to 274˚C, with an average which is 19˚C lower than the water temperatures.

As already pointed out, the aquifer water in both geothermal systems may have been affected by loss of Ar and H_2 by boiling and steam separation, and less so by some loss of the more soluble CO_2.

H_2-CO_2 and H_2S-CO_2 geothermometers
In wells of Ahuachapán and Berlín fields, the H_2-CO_2 geothermometer temperatures are much lower than the water temperatures, ranging from 113 to 220˚C and from 163 to 215˚C, respectively. Here again the low temperatures estimated may be affected by the depletion of H_2 in the aquifer fluid.

In Ahuachapán, the H_2S-CO_2 geothermometer yields values from 207 to 252˚C, but the Berlín wells give temperatures ranging from 252 to 263˚C.

CO_2, H_2S, H_2, CO_2/H_2 and H_2S/H_2 geothermometers
The H_2S geothermometer yields values in the range from 247 to 275˚C, and from 280 to 286˚C, for Ahuachapán and Berlín, respectively. In both fields, the rest of the geothermometers show higher deviation from the average of the three water geothermometers.

TABLE 8: Gas and water geothermometers for Ahuachapán and Berlín geothermal wells

Well	Gas geothermometers (°C)													Gas geothermometers (°C)					ΔT gases - waters (°C)
	D'Amore [a]	(H₂/Ar) [b]	CO₂/Ar [b]	CH₄/CO₂ [b]	CO₂ [c]	H₂S [c]	H₂ [c]	CO₂/H2 [c]	H₂S/H₂ [c]	H₂-CO₂ [d]	H₂S-CO₂ [d]	Standard Deviation	Average [e]	SiO₂ [f]	Average Na/K [g]	Na-K-Ca [h]	Standard Deviation	Average	
AH-4BIS	207	241	275	392	259	258	257	259	257	192	227	25	243	222	240	228	9	230	+13
AH-6	225	272	289	413	275	275	265	264	257	220	252	21	259	210	248	227	19	228	+31
AH-16A	208	249	277	347	233	254	253	261	252	171	219	29	238	241	265	252	12	252	-15
AH-17	202	241	293	436	266	275	251	248	231	179	250	32	244	-	-	-	-	-	-
AH-19	227	225	265	404	177	248	240	259	234	124	207	40	221	224	232	228	4	228	-7
AH-20	219	244	279	427	216	247	247	258	246	151	209	34	232	215	243	235	14	231	+1
AH-21	208	242	286	416	233	257	247	253	238	155	223	33	234	227	249	243	11	239	-5
AH-22	217	232	268	405	232	253	251	260	250	167	218	28	235	218	240	230	11	229	+6
AH-23	195	221	271	395	275	266	258	253	251	198	239	27	243	223	246	234	11	234	+9
AH-26	211	255	286	407	270	268	260	258	253	203	242	25	251	214	241	230	14	228	+23
AH-27	201	243	284	392	261	263	255	255	248	185	234	28	243	247	266	253	10	255	-13
AH-28	210	218	279	455	194	249	235	248	223	113	209	42	218	232	267	251	17	250	-32
AH-33B	214	237	277	417	245	262	252	256	243	173	231	28	239	226	250	247	13	241	-2
AH-35A	197	211	281	455	248	266	243	243	222	149	237	36	230	218	223	222	3	221	+9
TR-2	256	240	261	387	215	283	253	267	227	167	256	31	243	278	289	274	8	280	-38
TR-4B	268	262	260	386	247	286	267	276	250	214	263	19	259	281	298	283	9	288	-28
TR-4C	287	268	254	378	235	285	269	283	255	215	260	22	261	281	284	271	7	278	-17
TR-5A	263	256	267	381	210	283	255	270	230	169	254	32	246	284	302	288	9	291	-46
TR-5B	266	249	261	398	217	281	256	271	234	176	253	29	247	283	298	280	9	287	-41
TR-5C	251	253	274	394	216	282	252	265	225	163	255	33	244	281	282	269	7	278	-34
TR-5V	254	242	262	385	225	285	255	267	229	176	259	29	245	290	300	289	6	293	-48
TR-9	260	263	274	402	218	280	255	269	233	173	252	31	248	276	278	263	8	273	-25

[a] D'Amore and Panichi, 1980; [b] Giggenbach, 1991; [c] Arnórsson and Gunnlaugsson, 1985; [d] Nehring and D'Amore, 1984;
[e] Average value includes all gas geothermometers except CH₄/CO₂; [f] Gudmundsson and Arnórsson, 2002;
[g] Average value of all 6 Na/K geothermometers detailed in Appendix 1; [h] Fournier, 1977.

TABLE 9: Difference between gas geothermometers and reference temperatures[1]
for Ahuachapán and Berlín geothermal wells

Well	D'Amore[a]	(H_2/Ar)[b]	(CO_2/Ar)[b]	(CH_4/CO_2)[b]	CO_2[c]	H_2S[c]	H_2[c]	(CO_2/H_2)[c]	(H_2S/H_2)[c]	$(H_2\text{-}CO_2)$[d]	$(H_2S\text{-}CO_2)$[d]	Average[e]
AH-4BIS	-23	+11	+45	+162	+29	+28	+27	+29	+27	-38	-3	+27
AH-6	-3	+44	+61	+185	+47	+47	+37	+36	+29	-8	+24	+45
AH-16A	-44	-3	+25	+95	-19	+2	+1	+9	0	-81	-33	-4
AH-17 [2]	-42	-3	+49	+192	+22	+31	+7	+4	-13	-65	+6	+17
AH-19	-1	-3	+37	+176	-51	+20	+12	+31	+6	-104	-21	+9
AH-20	-12	+13	+48	+196	-15	+16	+16	+27	+15	-80	-22	+18
AH-21	-31	+3	+47	+177	-6	+18	+8	+14	-1	-84	-16	+12
AH-22	-12	+3	+39	+176	+3	+24	+22	+31	+21	-62	-11	+21
AH-23	-39	-13	+37	+161	+41	+32	+24	+19	+17	-36	+5	+23
AH-26	-17	+27	+58	+179	+42	+40	+32	+30	+25	-25	+14	+37
AH-27	-54	-12	+29	+137	+6	+8	0	0	-7	-70	-21	+1
AH-28	-40	-32	+29	+205	-56	-1	-15	-2	-27	-137	-41	-11
AH-33B	-27	-4	+36	+176	+4	+21	+11	+15	+2	-68	-10	+14
AH-35A	-24	-10	+60	+234	+27	+45	+22	+22	+1	-72	+16	+29
Average	-26	+2	+43	+175	+5	+24	+15	+19	+7	-66	-8	+17
Num. average	26	13	43	175	26	24	17	19	14	66	17	19
Std Dev.	16	18	12	32	33	15	14	13	16	33	19	15
TR-2	-24	-40	-19	+107	-65	+3	-27	-13	-53	-113	-24	-38
TR-4B	-20	-26	-28	+98	-41	-2	-21	-12	-38	-74	-25	-29
TR-4C	+9	-10	-24	+100	-43	+7	-9	+5	-23	-63	-18	-17
TR-5A	-28	-35	-24	+90	-81	-8	-36	-21	-61	-122	-37	-45
TR-5B	-21	-38	-26	+111	-70	-6	-31	-16	-53	-111	-34	-41
TR-5C	-27	-25	-4	+116	-62	+4	-26	-13	-53	-115	-23	-34
TR-5V	-39	-51	-31	+92	-68	-8	-38	-26	-64	-117	-34	-48
TR-9	-13	-10	+1	+129	-55	+7	-18	-4	-40	-100	-21	-25
Average	-20	-29	-19	+105	-61	0	-26	-13	-48	-102	-27	-35
Num. average	23	29	20	105	61	6	26	14	48	102	27	35
Std Dev.	14	14	12	13	14	6	10	10	14	22	7	10

[a] D'Amore and Panichi, 1980;   [b] Giggenbach, 1991;   [c] Arnórsson and Gunnlaugsson, 1985;
[d] Nehring and D'Amore, 1984;   [e] Average value includes all gas geothermometers except CH_4/CO_2;
[1] Average of three water geothermometers (quartz, Na/K and Na/K/Ca);
[2] Reference temperature, 207°C, from logging measurements

The calibration of these geothermometers is geochemical and based on the observed concentration variations of CO_2, H_2S and H_2 in well discharges with aquifer temperature in different geothermal fields.

Figures 5 and 6 show the geothermometer temperatures plotted against the respective average of water temperatures for both the Ahuachapán and Berlín fields.

6.3.2 New fitting of steam geothermometers based on CO_2, H_2, H_2S mineral-gas equilibria

Because of the difference in temperature values obtained with water and gas geothermometers, respectively, an attempt was made to derive gas geothermometry equations for the CO_2, H_2, and H_2S geothermometers that are consistent with the composition of minerals in the respective geothermal systems which are likely to participate in the respective mineral – gas equilibria.
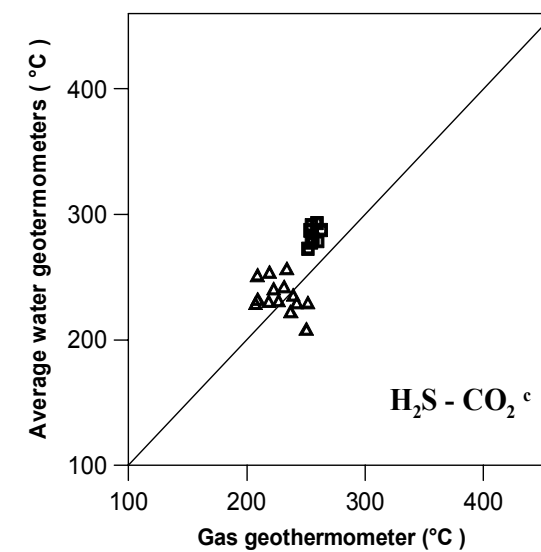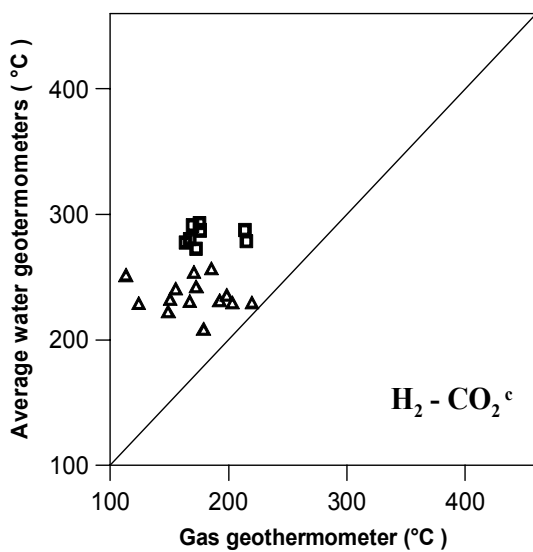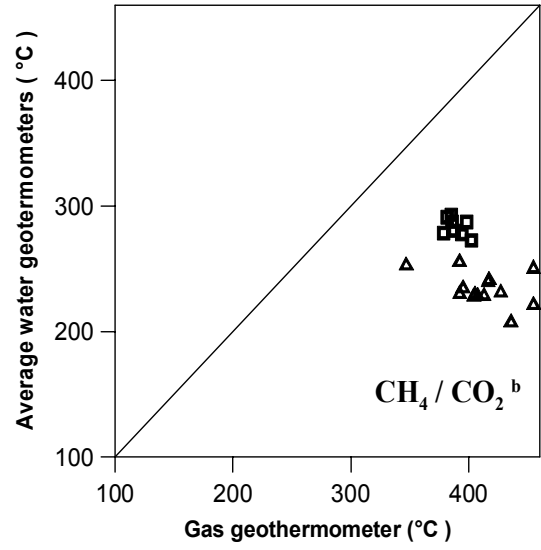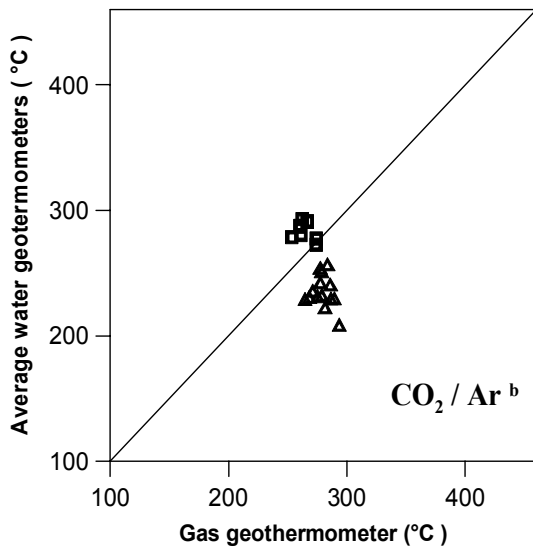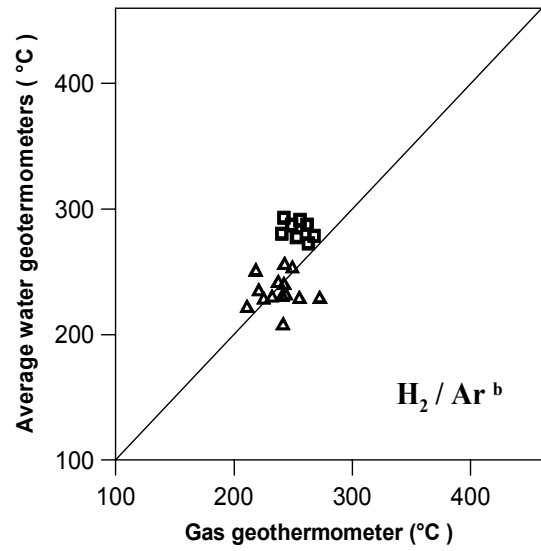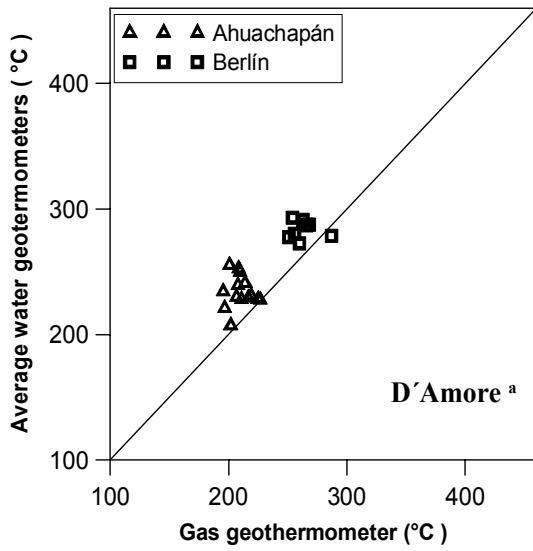
FIGURE 5: Temperatures based on gas geothermometer results, [a]D'Amore and Panichi, 1980; [b]Giggenbach, 1991; [c]Nehring and D'Amore, 1984; the values are plotted against the average of the three water geothermometers, quartz, Na/K, Na/K/Ca (Table 8)
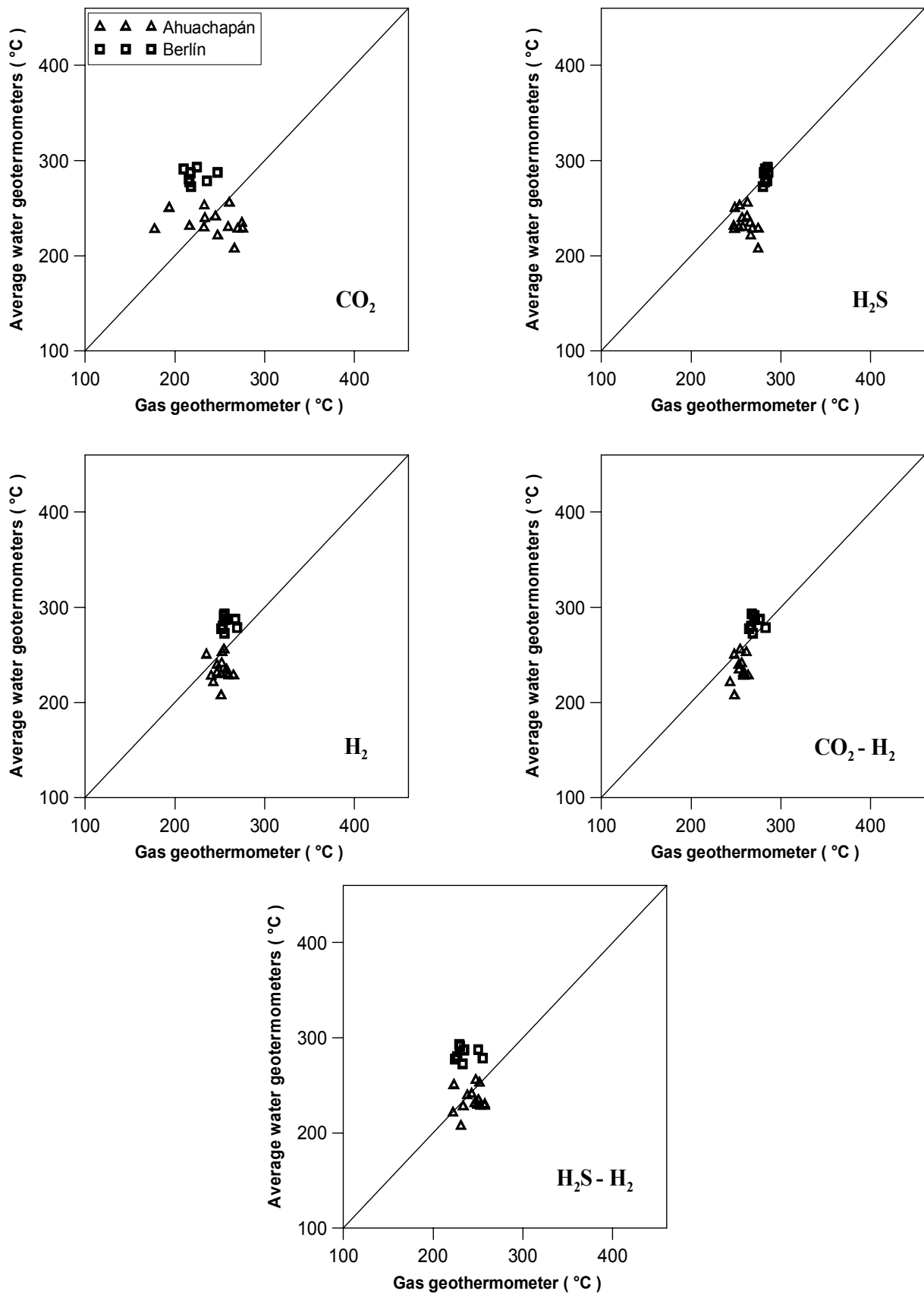
FIGURE 6:   Temperatures based on gas geothermometer results from Arnórsson and Gunnlaugsson (1985); the values are plotted against the average of the three water geothermometers, quartz, Na/K, Na/K/Ca (Table 8)

According to Arnórsson and D'Amore (2000), the selection of an equation describing the temperature dependence of aqueous gas concentrations should, as far as possible, be based on data on alteration mineralogy in the geothermal system in question, and on calculation of the equilibrium constant for the respective gas-mineral reaction from the thermodynamic properties of the gases and minerals involved.

The temperature equations for CO_2, H_2, H_2S mineral-gas equilibria geothermometers are based on thermodynamic data for the following reactions (Arnórsson et al., 1998):

$$Ca_2Al_3Si_3O_{12}(OH) + CaCO_3 + \tfrac{3}{2}SiO_2 + H_2O = \tfrac{3}{2}Ca_2Al_2Si_3O_{10}(OH)_2 + CO_{2,aq} \qquad (11)$$

$$\tfrac{1}{3}FeS_2 + \tfrac{1}{3}FeS + \tfrac{2}{3}Ca_2Al_2Si_3O_{10}(OH)_2 + \tfrac{2}{3}H_2O = \tfrac{2}{3}Ca_2Al_3Si_3O_{12}(OH) + H_2S_{aq} \quad (12)$$

$$\tfrac{4}{3}FeS + \tfrac{2}{3}Ca_2Al_2Si_3O_{10}(OH)_2 + \tfrac{2}{3}H_2O = \tfrac{2}{3}Ca_2Al_3Si_3O_{12}(OH) + \tfrac{2}{3}FeS_2 + 3H_{2,aq} \qquad (13)$$

Alteration mineralogy in the Berlín and Ahuachapán fields (Table 1; Table 2) indicates the presence of the minerals included in Reactions 11-13. On this basis, the above reactions can be applied.

According to Karingithi (2002), for reservoir waters, the gas geothermometry temperature equations for the above reactions are:

$$\log CO_2 = k_o - 1.297 - 771.80/T + 0.007134\,T - 0.310\log T \qquad (14)$$

$$\log H_2S = k_o - 0.481 - 3129.34/T + 0.005705\,T + 0.187\log T \qquad (15)$$
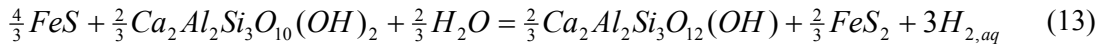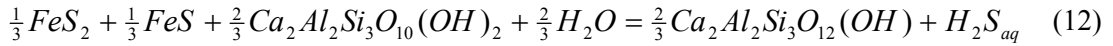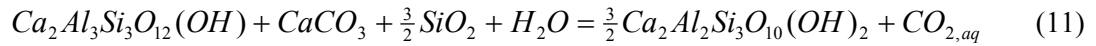
$$\log H_2 = k_o - 2.411 - 1296.88/T + 0.006830\,T - 0.725\log T \qquad (16)$$

In these equations, the value of k_o is determined by the composition (activity) of the minerals with which the respective gases equilibrate. By taking clinozoisite and epidote activities to be 0.02 and 1, respectively, gas concentrations were fitted to yield the following equations:

$$t°C\ (CO_2) = -492.2 + 785.5Q - 297.42Q^2 + 46.099Q^3 \qquad (17)$$

$$t°C\ (H_2S) = 211.9 + 66.423Q + 2.317Q^2 + 1.437Q^3 \qquad (18)$$

$$t°C\ (H_2) = +219.2 + 132.49Q - 18.152Q^2 + 17.949Q^3 \qquad (19)$$

where Q represents the logarithm of the respective gas concentration in mmoles/kg of steam at 1 bar assuming that the aquifer water, is boiled in one step from the respective gas geothermometer temperature to 1 bar (100°C).

Aquifer temperatures for the Ahuachapán and Berlín production fields were calculated by Equations 17-19 as shown in Table 10, together with results for the same geothermometers as calibrated by Arnórsson et al. (1998) (Appendix I); as well as the average of three water geothermometers, quartz, Na/K, Na/K/Ca. For Ahuachapán, the new H_2S-geothermometer calibration gives, on average, a temperature value which is close to the average of the water geothermometers. On the other hand, CO_2- and H_2-temperatures are lower and much lower, respectively. The very low H_2-temperatures can be accounted for by the presence of secondary steam in the well discharges. In the case of Berlín, the new calibration for all the gas geothermometers gives substantially lower values than those of the water geothermometers, particularly in the case of the H_2-geothermometer. Again the discrepancy can be explained by the presence of secondary steam in well discharges.

Calculated Ar concentrations in the aquifers of wells at Ahuachapán and Berlín are as much as 10 times lower than in air-saturated water. This result substantiates the interpretation for the gas geothermometers. Hydrogen being less soluble than Ar would be even more depleted. Depletion to 10% of the initial H_2 concentration would lower H_2-temperatures by some 80°C.

TABLE 10:   Gas geothermometers temperatures (in ˚C)
based on CO_2, H_2S and H_2 mineral-equilibria

Well	T_{ref} [a]	CO_2 [b]	H_2S [b]	H_2 [b]	CO_2 [c]	H_2S [c]	H_2 [c]
AH-4BIS	230	255	194	174	251	228	64
AH-6	228	274	221	196	284	255	136
AH-16A	252	231	189	159	200	223	11
AH-17	207	263	221	155	265	255	-5
AH-19	228	197	180	110	86	214	-168
AH-20	231	219	179	138	168	213	-64
AH-21	239	232	193	138	201	227	-66
AH-22	229	231	188	154	199	222	-5
AH-23	234	273	206	174	282	240	64
AH-26	228	268	210	181	273	244	88
AH-27	255	257	202	165	254	236	34
AH-28	250	205	181	83	121	215	-270
AH-33B	241	242	201	156	224	235	0
AH-35A	221	244	208	120	229	242	-131
Average	234	242	198	150	217	232	-22
TR-2	280	218	235	161	166	269	17
TR-4B	288	243	240	200	228	273	149
TR-4C	278	233	237	206	205	271	163
TR-5A	291	215	234	165	155	267	32
TR-5B	287	220	232	170	169	265	51
TR-5C	278	219	233	155	168	267	-3
TR-5V	293	225	238	167	184	271	41
TR-9	273	220	229	166	171	263	37
Average	284	224	235	174	181	268	61

a) Average temperature estimated with quartz, Na/K and Na/K/Ca geothermometers (Table 8);
b) Arnórsson et al., 1998; this approach assumes clinozoisite and epidote activities of 0.3 and 0.7, respectively, but unit activity for all other minerals and water;
c) New fitted equation based on Karingithi, 2002; this approach assumes clinozoisite and epidote activities of 0.02 and 1 respectively, but unit activity for all other minerals and water.

6.4 Steam fraction

The initial steam fraction in producing aquifers was estimated by two methods, *Model I* (D'Amore, 1998) and *Model II* (Arnórsson et al., 1990).

By *Model I*, wells in the Ahuachapán field have initial steam weight fraction of – 0.7 to 3.0%. The corresponding percentage volume of steam ranges from -30.0 to 65.5%. Aquifer temperature estimations for wells AH-19, AH-20, AH-21 and AH-27 are very close to the average of the water geothermometers. However, the rest of the wells have lower or higher values. In the Berlín field, the majority of the wells show a close correspondence between aquifer temperature estimations and the average of the water geothermometers, with initial steam fractions in the range -1 to +1% by weight (Figure 7 and Table 11).

According to *Model II*, Ahuachapán and Berlín wells have low initial steam weight fraction, ranging from -0.075 to -0.599%. The calculated Y_{HS} and Y_{HC} values by this model show good correlation yet systematically negative, and they agree in the sense that they indicate that the initial steam fractions in the aquifers of both geothermal reservoirs are low and only a minor fraction of the reservoir fluid, even in terms of volume (Table 11).
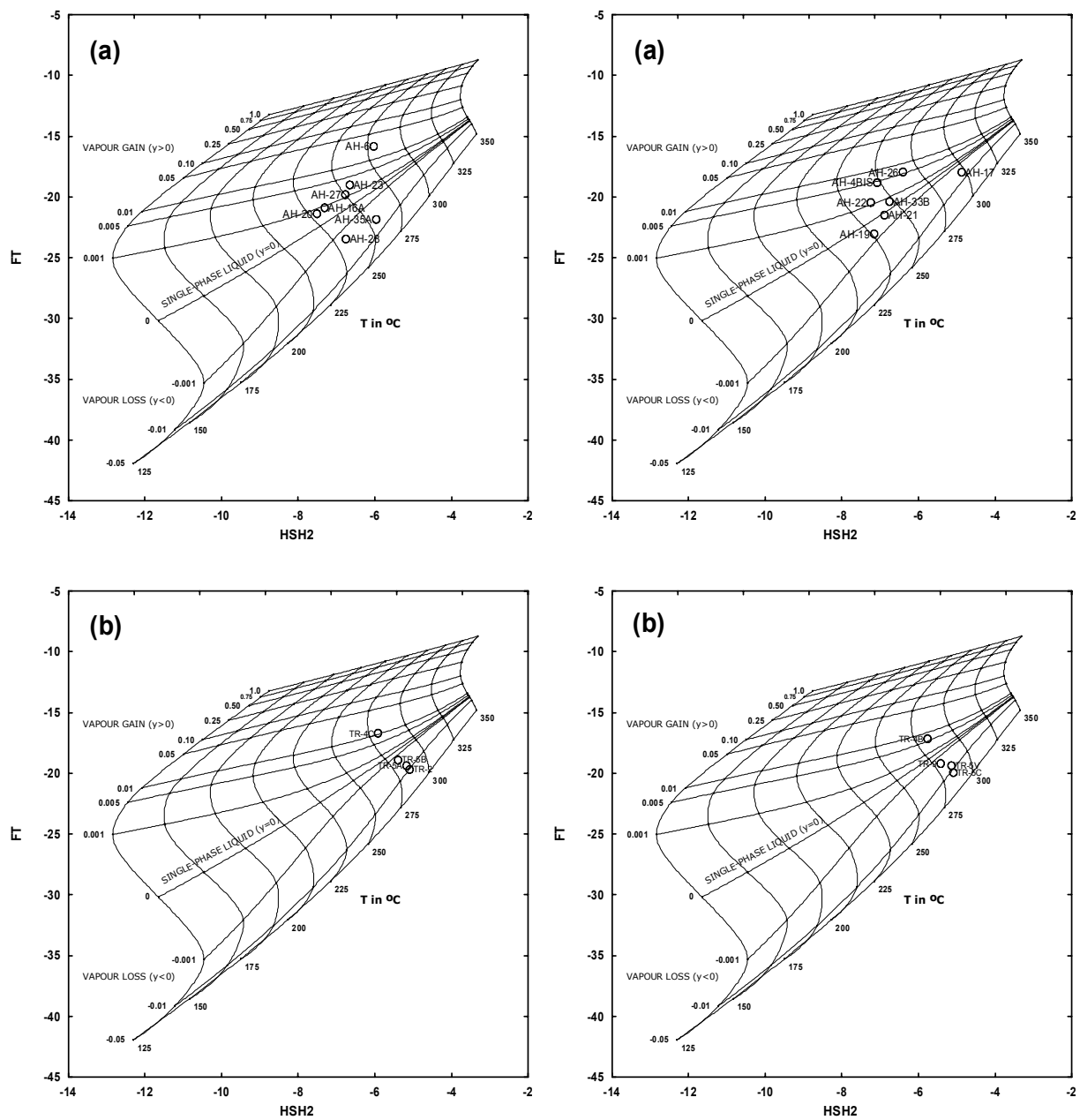
FIGURE 7: Initial aquifer steam fraction by Model I, a) the Ahuachapán wells; b) the Berlín wells

Model I.
This model estimates both the reservoir temperature and the excess steam based on equilibrium for the Fischer-Tropsch reaction and, the two chemical reactions for H_2S-H_2: a pyrite-magnetite and a pyrite-hematite equilibria. Of these reactions, it is known that the Fischer-Tropsch reaction takes a long time for equilibration, possibly longer than the residence time of the fluid in the respective reservoirs, i.e the CO_2/CH_4 redox equilibrium is not closely approached in these reservoirs. This lack of equilibrium may be responsible for the few relatively high values of excess of steam computed by Model I, because most wells in the Ahuachapán and Berlín geothermal fields have liquid enthalpy.

Model II.
The Y_{HC} and Y_{HS} values depend on the gas content of the steam discharged from the well, the values selected for the aquifer temperature, and the thermodynamic data selected to describe the gas solubilities. According to Arnórsson et al. (1990), the value obtained for *Y* is very sensitive to the value selected for

TABLE 11: Initial steam fraction in the aquifer fluid on individual Ahuachapán and Berlín wells

Well	T_{ref}[a] (°C)	P_{aq}[b] (bar-a)	Discharge enthalpy (kJ/kg)	Excess enthalpy (kJ/kg)	P_s[c] (bar-a)	X_s	Model I[d]				Model II[e]			
							T (°C)	Y	% Y (w/w)	% Y (v/v)	% Y_{HS} (w/w)	% Y_{HC} (w/w)	% Y_{HS} (v/v)	% Y_{HC} (v/v)
AH-4BIS	230	28.0	1349	359	7.0	0.32	248	0.005	0.5	22.9	-0.093	-0.099	-5.2	-5.6
AH-6	228	27.0	2114	1133	6.4	0.69	280	0.03	3	65.5	-0.088	-0.094	-5.1	-5.5
AH-16A	252	41.1	1061	-35	6.9	0.18	234	0.001	0.1	3.7	-0.181	-0.188	-6.5	-6.8
AH-17	244	35.9	2734	1677	10.6	0.98	297	-0.007	-0.7	-24.0	-0.148	-0.150	-6.2	-6.3
AH-19	228	27.0	914	-67	8.2	0.09	226	-0.0008	-0.08	-4.7	-0.092	-0.094	-5.4	-5.5
AH-20	231	28.5	978	-17	6.4	0.14	229	0.0007	0.07	3.9	-0.099	-0.102	-5.4	-5.6
AH-21	239	32.9	978	-55	6.5	0.14	238	-0.0002	-0.02	-1.0	-0.127	-0.129	-5.9	-6.0
AH-22	229	27.5	1079	93	6.8	0.19	237	0.001	0.1	5.7	-0.093	-0.097	-5.3	-5.5
AH-23	234	30.1	1231	222	6.4	0.26	256	0.003	0.3	14.1	-0.107	-0.112	-5.5	-5.8
AH-26	228	27.0	1491	510	6.6	0.39	267	0.005	0.5	23.6	-0.089	-0.094	-5.2	-5.5
AH-27	255	43.2	1135	25	6.4	0.22	250	0.001	0.1	3.5	-0.199	-0.205	-6.7	-7.0
AH-28	250	39.8	955	-131	6.4	0.13	232	-0.003	-0.3	-10.7	-0.176	-0.178	-6.6	-6.6
AH-33B	241	34.1	1026	-16	7.3	0.16	248	0.005	0.5	19.3	-0.134	-0.137	-6.0	-6.1
AH-35A	221	23.6	1003	55	7.6	0.14	254	-0.006	-0.6	-30.0	-0.075	-0.076	-5.1	-5.1
TR-2	280	64.2	1348	111	12.5	0.27	284	-0.01	-1	-18.6	-0.413	-0.417	-8.6	-8.6
TR-4B	288	72.3	1307	28	14.5	0.24	283	0.007	0.7	12.0	-0.505	-0.522	-9.0	-9.2
TR-4C	278	62.3	1379	153	11.9	0.29	280	0.01	1	19.2	-0.375	-0.394	-8.1	-8.5
TR-5A	291	75.6	1419	124	13.3	0.31	283	-0.008	-0.8	-12.9	-0.561	-0.567	-9.4	-9.5
TR-5B	287	71.3	1381	107	13.4	0.29	282	-0.008	-0.8	-13.8	-0.500	-0.507	-9.1	-9.2
TR-5C	278	62.3	1332	106	13.5	0.26	283	-0.015	-1.5	-26.3	-0.391	-0.394	-8.4	-8.5
TR-5V	293	77.8	1312	6	11.7	0.26	284	-0.008	-0.8	-12.5	-0.594	-0.599	-9.5	-9.6
TR-9	273	57.7	1361	160	13.8	0.27	280	-0.003	-0.3	-7.2	-0.338	-0.342	-8.0	-8.1

[a] Average temperature estimated with quartz, Na/K and Na/K/Ca geothermometers (Table 8);
[b] Pressure of saturated steam at the aquifer temperature, from steam tables;

the aquifer temperature and the selection of too high an aquifer temperature for a well gives too low Y values and vice versa. In the present study, the values for $m^{f,\,l}_g$ (the concentrations of CO_2, H_2S and H_2 in the reservoir water) were obtained from chemical thermodynamic data temperature functions given by Karingithi (2002) (Table 6). This approach assumes that the gaseous species are controlled by reactions given in Table 8. As a result, lack of equilibrium for those reactions will affect the reliability of the values for $m^{f,\,l}_g$. Moreover, the type and composition of alteration minerals with which the gases tend to equilibrate in the reservoir rock may be different, and the computed Y values could be systematically in error. For more reliable interpretation of the gas data, it would be important to get more information on the type and composition of the alteration minerals in the reservoir rock.

The low Y values estimated for high enthalpy wells, such as AH-6, could be explained by long-term extensive boiling in the reservoir around discharging wells and the presence of secondary steam in the discharge. Alternatively, partial re-equilibration between gases and minerals in the disturbed zone may be responsible. Such re-equilibration would tend to remove H_2S and H_2 from the steam relative to CO_2 (Arnórsson and Gunnlaugsson, 1985).

7. DISCUSSION AND CONCLUSIONS

The gas composition of geothermal fluids can be used to estimate sub-surface conditions such as temperature and steam fraction beyond the depressurization zone. Because the models are constrained by several assumptions, they cannot be expected to apply equally well to all geothermal systems. Data interpretation must be based on assessing the validity of the assumptions made.

The aquifer fluids from wells in the Ahuachapán and Berlín fields show relatively low total gas content. The computed concentrations of N_2 and Ar indicate the presence of secondary steam component in the well discharges. The high N_2/Ar ratios are considered to be the consequence of a supply of N_2 to the aquifer fluid.

In the Ahuachapán wells, the average temperatures of all the gas geothermometers differ from the average of the water geothermometers from -32°C to +31°C. For Berlín wells, all gas geothermometers yield low temperature values. Of the fourteen geothermometers, those based on H_2S and CO_2 concentrations yield the best results. As already pointed out, the fluid discharged from wells at present appears to be affected by the presence of secondary steam which would cause it to be low in sparingly soluble gases, such as Ar and H_2.

Geothermometer results may also be affected by departure from equilibria. This could explain the high temperatures indicated by the Fisher-Tropsch geothermometer (a very slow reaction) as well as the low values estimated by the multi-component system CH_4/CO_2/H_2/H_2S. Moreover, several factors other than aquifer temperature and departure from chemical equilibrium may affect the gas composition of a geothermal well discharge, e.g. the steam to water ratio in the discharge at a given separation pressure, mixing processes in upflow zones and inflow of gases into geothermal systems from their magmatic heat source. Such factors may be quite significant and influence how closely gas-gas and mineral-gas equilibria are approached in specific aquifers.

The computed Y values indicate that the initial steam fractions in the aquifers of both Ahuachapán and Berlín geothermal reservoirs are low and generally negative, i.e. the aquifer water flowing into wells has lost some steam. Alternatively, the low gas content could be the consequence of recharge of cold, gas-depleted water.

ACKNOWLEDGEMENTS

REFERENCES

Arnórsson, S., 2000: The quartz and Na/K Geothermometers. I. New thermodynamic calibration. *Proceedings World Geothermal Congress 2000, Kyushu – Tohoku, Japan*, 929-934.

Arnórsson, S., and D'Amore, F., 2000: Estimation of aquifer steam fraction. In: Arnórsson, S. (ed.), *Isotopic and chemical techniques in geothermal exploration, development and use. Sampling methods, data handling, interpretation.* International Atomic Energy Agency, Vienna, 267-308.

Arnórsson, S., and Gunnlaugsson, E., 1985: New gas geothermometers for geothermal exploration – calibration and application. *Geochim. Cosmochim. Acta, 49*, 1307-1325.

Arnórsson, S., Björnsson, S., Muna, Z.W., Bwire-Ojiambo, S., 1990: The use of gas chemistry to evaluate boiling processes and initial steam fractions in geothermal reservoirs with an example from the Olkaria field, Kenya. *Geothermics, 19,* 497-514.

Arnórsson, S., Fridriksson, T., and Gunnarsson, I., 1998: Gas chemistry of the Krafla Geothermal Field, Iceland. In: Arehart G., and Hulston, J. (ed.), *Water-Rock interaction IX.* Balkema, Rotterdam, 613-616.

Arnórsson, S., Gunnlaugsson, E., and Svavarsson, H., 1983: The chemistry of geothermal waters in Iceland. III. Chemical geothermometry in geothermal investigations. *Geochim. Cosmochim. Acta, 47*, 567-577.

Barragán, R.M., Arellano, V.M., Nieva, D., Portugal, E., García, A., Aragón, A., Tovar, R., and Torres-Alvarado, I., 2000: Gas chemistry of the Los Humeros geothermal field, México. *Proceedings of the World Geothermal Congress 2000, Kyushu-Tohoku, Japan*, 2527-2532.

Barragán, R.M., Arellano, V.M., Portugal, E., and Sandoval, F., 2003: Gas chemistry for the Los Azufres (Michoacán) geothermal reservoir, México. *Proceedings of the 7th International Conference on Gas Geochemistry 2003*, Germany, 15-17.

CEL, 1997: *Conceptual model of the Ahuachapán geothermal field*. CEL, Gerencia de Recursos Geotérmicos, internal report (in Spanish), 197 pp.

D'Amore, F., 1998: *Time evolution of chemical and physical parameters of the reservoir fluid in Ahuachapán geothermal field (El Salvador)*.International Atomic Energy Agency, Vienna, report, 210 pp.

D'Amore, F., and Arnórsson, S., 2000: Geothermometry. In: Arnórsson, S. (ed.), *Isotopic and chemical techniques in geothermal exploration, development and use. Sampling methods, data handling, interpretation*. International Atomic Energy Agency, Vienna, 152-199.

D'Amore, F., and Mejía, J.T., 1999: Chemical and physical reservoir parameters at initial conditions in Berlin geothermal field El Salvador: A first assessment. *Geothermics, 28,* 45-73.

D'Amore, F., and Panichi, C., 1980: Evaluation of deep temperatures in hydrothermal systems by a new gas geothermometer. *Geochim. Cosmochim. Acta, 44,* 549-556.

D'Amore, F., and Truesdell, A.H., 1985: Calculation of geothermal reservoir temperatures and steam fractions from gas compositions. *Geothermal Resources Council, Trans., 9,* 305-310.

Duffield, W.A., Heiken, G.H., Wohletz, K.H., Maassen, L.W., Dengo, G., and McKee, E.H., 1989: Geology and geothermal potential of the Tecuamborro volcano area of Guatemala. *Geothermal Resources Council, Trans., 13,* 305-310.

Faure, G., 1991: *Principles and applications of inorganic geochemistry.* Prentice-Hall, New Jersey, United States of America, 626 pp.

Fournier, R.O., 1977: Chemical geothermometers and mixing models for geothermal systems. *Geothermics, 5*, 41-50.

Fournier, R.O., 1991: Water geothermometers applied to geothermal energy. In: D'Amore, F. (coordinator), *Application of geochemistry in geothermal reservoir development.* UNITAR/UNDP publication, Rome, 37-69.

GESAL, 2000: *Updated conceptual model of the Berlín geothermal field.* GESAL, Gerencia de Proyectos, internal report (in Spanish), 19 pp.

Giggenbach, W.F., 1988: Geothermal solute equilibria. Derivation of Na-K-Ca geoindicators. *Geochim. Cosmochim. Acta*, 52, 2749-2765.

Giggenbach, W.F., 1991: Chemical techniques in geothermal exploration. In: D'Amore, F. (coordinator), *Application of geochemistry in geothermal reservoir development.* UNITAR/UNDP publication, Rome, 119-142.

Gudmundsson, B.T., and Arnórsson, S., 2002: Geochemical monitoring of the Krafla and Námafjall geothermal areas, N-Iceland. *Geothermics, 31,* 195-243.

Karingithi, C., 2002: *Hydrothermal mineral buffers controlling reactive gases concentration in the Greater Olkaria geothermal system, Kenya.* University of Iceland, MSc. thesis, UNU-GTP, Iceland, report 2, 94 pp.

Montalvo, F.E., 1994: Geochemical evolution of the Ahuachapán geothermal field, El Salvador. Report 9 in: *Geothermal Training in Iceland 1994.* UNU-GTP, Iceland, 211-236.

Nehring, N.L., and D'Amore, F., 1984: Gas chemistry and thermometry of the Cerro Prieto, Mexico, geothermal field, *Geothermics, 13,* 75-89.

Nicholson, K., 1993: *Geothermal fluids. Chemistry and exploration techniques.* Springer-Verlag, Berlin, Germany, 263 pp.

Quijano, J.E., 1994: A revised conceptual model and analysis of production data for the Ahuachapán-Chipilapa geothermal field in El Salvador. Report 10 in: *Geothermal Training in Iceland 1994.* UNU-GTP, Iceland, 237-266.

Renderos, R., 2002: Chemical characterization of the thermal fluid discharge from well production tests in the Berlín geothermal field, El Salvador. Report 12 in: *Geothermal Training in Iceland 2002*. UNU-GTP, Iceland, 205-232.

Truesdell, A.H., 1976: Summary of section III - geochemical techniques in exploration. *Proceedings of the 2nd U.N. Symposium on the Development and Use of Geothermal Resources, San Franc., 1,* liii-lxxix.

APPENDIX I: Temperature equations for gases and water geothermometers

TABLE 1:   Temperature equations for gas geothermometers;
gas concentrations are in log mmoles per kg of steam at 1 bar

Geothermometer	Equation	Reactions / calibrations	Temperature range (˚C)	Source
D'Amore and Panichi[a, e]	$t^oC = \dfrac{24775}{\alpha + \beta + 36.05} - 273.15$	$C + CO_2 + 6\,H_2 = 2\,CH_4 + 2\,H_2O$ $CaSO_4 + FeS_2 + 3\,H_2O =$ $CaCO_3 + 1/3\,Fe_3O_4 + 3\,H_2S + 7/3\,O_2$	-	1
$H_2\text{-}CO_2$[b, f]	$t\ ^\circ C = 190.3 + 55.97\,Q_{HC} - 0.14\,Q_{HC}^2$	$H_2 + \frac{1}{2}\,O_2 = H_2O$ $C + O_2 = CO_2$	-	2
$H_2S\text{-}CO_2$[b, g]	$t\ ^\circ C = 194.3 + 56.44\,Q_{SC} - 1.53\,Q_{SC}^2$	$3FeS_2 + 2G_2 + 4G_2O = Fe_3O_4 + 6H_2S$ $C + O_2 = CO_2$	-	2
CO_2[b, d]	$t\ ^\circ C = 44.1 + 269.25\,Q - 76.88\,Q^2 + 9.52\,Q^3$	-	100-330	3
H_2S[b, d]	$t\ ^\circ C = 246.7 + 44.81\,Q$	-	> 200	3
H_2[b, d]	$t\ ^\circ C = 277.2\ + 20.99\,Q$	-	> 200	3
CO_2 / H_2[b, d]	$t\ ^\circ C = 341.7 + 28.57\,Q$	-	> 200	3
H_2S / H_2[b, d]	$t\ ^\circ C = 304.1 + 39.48\,Q$	-	> 200	3
H_2 / Ar[c]	$t\ ^\circ C = 70\,(2.5 + \log (H_2 / Ar))$	Ferrous / ferric ratio in the rock fixes the H_2/H_2O fugacity ratio, Ar content of air-saturated groundwater at 25˚C	-	4
CO_2 / Ar[c, h]	$\log (CO_2/Ar) = 0.0277\,t - 7.53 + 2048 / (t+273)$	$CaAl_2\text{-}silicate + K\text{-}feldspar + CO_2 = K\text{-}mica + calcite$ Ar content of air-saturated groundwater at 25˚C	-	4
CH_4 / CO_2[c]	$t^oC = \dfrac{4625}{10.4 + \log(CH_4/CO_2)} - 273.15$	$CO_2 + 4\,H_2 = CH_4 + 2\,H_2O$	> 300	4
CO_2[b, d]	$t\ ^\circ C = 121.8 + 72.012Q - 11.068\,Q^2 + 4.724\,Q^3$	$czo. + calcite + 1.5\ quartz + H_2O$ $1.5\ prehnite + CO_{2\ aq}$	> 230	5
H_2S[b, d]	$t\ ^\circ C = 177.6 + 66.152\,Q - 4.811\,Q^2$	$1/3\ pyr. + 1/3\ pyrr. + 2/3\ pre.+ 2/3\ H_2O = 2/3\ epidote + H_2S$	> 150	5
H_2[b, d]	$t\ ^\circ C = 227.1 + 56.168\,Q - 5.836\,Q^2 + 6.630\,Q^3$	$4/3\ pyr. + 2/3\ pyrr. + 2/3\ H_2O = 2/3\ epidote + 2/3\ pyr + H_2$	> 150	5

1) D´Amore and Panichi, 1980;   2) Nehring and D'Amore, 1984;   3) Arnórsson and Gunnlaugsson, 1985;
4) Giggenbach, 1991;   5) Arnórsson et al., 1998.
a) Gas concentration in vol. %;   b) Gas concentration in log (mmol/kg);   c) Gas concentration in mole %;
d) Q = logarithm of the respective gas concentration or gas ratio;
e) $\alpha = 2\log CH_4/CO_2 - 6\log H_2 / CO_2 - 3\log H_2S/CO_2$ and $\beta = 7\log P_{CO2}$;
f) $Q_{HC} = \log H_2 + \frac{1}{2}\log CO_2$;   g) $Q_{SC} = \log H_2S + \frac{1}{6}\log CO_2$;   h) $t = ˚C$.

TABLE 2:   Temperature equations for water geothermometers
(concentrations are in ppm if not otherwise specified)

Geothermometer	Equation	Range (˚C)	Source
SiO_2^a	$127.18 + 48.11\,Q + 82.135\,Q^2$	> 180	Gudmundsson and Arnórsson, 2002
$Na\text{-}K$	$\dfrac{856}{0.857 + \log(Na/K)} - 273.15$	100 - 275	Truesdell, 1976
$Na\text{-}K$	$\dfrac{1217}{1.438 + \log(Na/K)} - 273.15$	-	Fournier, 1991
$Na\text{-}K$	$\dfrac{933}{0.993 + \log(Na/K)} - 273.15$	25-250	Arnórsson et al., 1983
$Na\text{-}K$	$\dfrac{1319}{1.699 + \log(Na/K)} - 273.15$	250-350	Arnórsson et al., 1983
$Na\text{-}K$	$\dfrac{1390}{1.750 + \log(Na/K)} - 273.15$	-	Giggenbach, 1988
$Na\text{-}K^b$	$733.6 - 770.551Y + 378.189Y^2 - 95.753Y^3 + 9.544Y^4$	-	Arnórsson, 2000
$Na\text{-}K\text{-}Ca^c$	$\dfrac{1647}{\log(Na/K) + \beta\log(Ca^{0.5}/Na) + 2.24} - 273.15$	-	Fournier, 1977

a) $Q = \log$ mmol / kg at 180˚C;   b) Y = molal ratio Na/K. for dilute to moderately saline waters below ˚C.
c) Concentrations are in mol/kg . $\beta = 4/3$ for $t < 100$˚C and 1/3 for $t > 100$˚C and for $\log(Ca^{0.5}/Na) < 0$.

APPENDIX II: Chemical data of geothermal fluids from Ahuachapán and Berlín wells

TABLE 1:   Chemical analysis of the fluid from Berlín wells; primary data[1]

Well	Date of sampling	$P_{sampling}$ (bar-a)	Water (ppm)				Steam (mmoles / 100 moles H_2O)						
			Na	K	Ca	SiO$_2$	He	H$_2$	Ar	N$_2$	CH$_4$	CO$_2$	H$_2$S
TR-2	13.04.02	12.7	3653	754	101	668	0.0004	0.2349	0.0208	1.5429	0.0313	82.89	15.72
TR-2	19.06.02	13.2	3642	796	106	746	0.0003	0.1678	0.0312	1.5819	0.0411	80.08	19.09
TR-2	27.09.02	11.6	3671	743	105	770	0.0003	0.1881	0.0182	1.4799	0.0251	75.05	18.97
TR-4B	19.06.02	14	2164	490	35	730	0.0005	0.8856	0.0905	4.0232	0.1229	192.39	22.63
TR-4B	19.09.02	15	2148	481	26	752	0.0006	1.0489	0.0344	3.3813	0.0501	181.68	22.14
TR-4C	26.04.02	11.5	3378	653	91	689	0.0008	1.0545	0.0526	3.4396	0.0763	125.15	14.31
TR-4C	19.06.02	12.5	3565	749	97	777	0.0004	1.5797	0.0603	2.5135	0.0561	121.08	19.55
TR-4C	19.09.02	11.7	3702	730	86	794	0.0005	0.7369	0.0411	2.5798	0.0528	120.32	22.67
TR-5A	18.06.02	12.0	2104	504	27	668	0.0007	0.2669	0.0114	2.4208	0.0466	71.21	17.93
TR-5A	00.01.00	14.5	2829	631	32	882	0.0005	0.1774	0.0201	1.7946	0.0216	64.80	15.15
TR-5B	18.06.02	12.6	3094	752	86	706	0.0007	0.3678	0.0244	2.0522	0.0225	73.60	16.84
TR-5B	18.09.02	14.2	3664	760	85	823	0	0.2043	0.024	1.9369	0.028	91.27	15.12
TR-5C	25.04.02	13.5	3941	730	140	756	0	0.2375	0.012	1.4721	0.025	81.44	17.81
TR-5C	18.06.02	13.6	3952	833	131	739	0	0.1226	0.014	1.1302	0.033	86.96	17.15
TR-5V	24.04.02	11.1	2594	577	30	799	0	0.2625	0.021	2.1462	0.038	98.96	22.1
TR-5V	13.06.02	12.9	2542	581	30	792	0	0.2025	0.041	2.2574	0.055	99.94	18.19
TR-5V	18.09.02	11	2590	611	29	889	0	0.2902	0.024	2.3001	0.036	96.77	18.81
TR-9	13.04.02	18.2	3629	653	127	656	0.0002	0.2633	0.0098	1.6778	0.022	100.71	14.75
TR-9	20.06.02	11.4	3839	788	156	756	0	0.1826	0.018	1.032	0.027	76.58	15.74
TR-9	26.09.02	11.8	3553	667	143	713	0.0003	0.297	0.014	1.0602	0.024	81.53	15.71

1) Samples collected at wellhead with a webre separator.

TABLE 2: Chemical analysis of the fluid from Ahuachapán wells; primary data

Well	Date of sampling	P_{sampl} (bar-a)	Water (ppm)				Steam (mmoles / 100 moles H_2O)						
			Na	K	Ca	SiO_2	He	H_2	Ar	N_2	CH_4	CO_2	H_2S
AH-4BIS[2]	10.04.02	7.4	3237	419	236	410	0.0020	0.2538	0.03	3.6411	0.063	196.76	5.72
AH-4BIS[2]	25.07.02	6.8	3508	452	270	428	0.0026	0.2832	0.0300	4.2216	0.0900	208.97	4.98
AH-4BIS[1]	13.11.02	7	3393	517	385	397	0.0026	0.2759	0.0331	4.3046	0.0751	227.56	2.43
AH-6[2]	26.07.02	6.4	4984	668	450	372	0.0012	0.4541	0.0227	2.6879	0.0567	288.44	10.40
AH-6[2]	12.11.02	6.4	5219	848	670	345	0.0018	0.6421	0.0211	3.8397	0.0720	291.95	6.67
AH-16A[2]	09.04.02	7.2	4954	788	321	537	0.0009	0.2160	0.0165	2.2021	0.1669	125.46	5.66
AH-16A[2]	12.11.02	6.6	5183	952	499	494	0.0009	0.1784	0.0175	2.0579	0.1249	127.03	3.13
AH-17[2]	22.03.02	11.3	-	-	-	-	0.0014	0.1592	0.0145	2.8500	0.0381	208.79	8.39
AH-17[1]	25.07.02	11.8	-	-	-	-	0.0010	0.0874	0.0135	2.3448	0.0333	204.71	8.85
AH-17[1]	03.09.02	10.4	-	-	-	-	0.0010	0.0853	0.0089	1.9128	0.0264	209.75	8.54
AH-17[2]	15.11.02	11.8	-	-	-	-	0.0009	0.0971	0.0121	2.0198	0.0242	197.21	8.78
AH-17[1]	15.11.02	11.4	-	-	-	-	0.0009	0.1601	0.0152	2.4988	0.0240	221.20	7.14
AH-17[2]	15.11.02	7.0	-	-	-	-	0.0009	0.1076	0.0127	2.2485	0.0234	206.51	6.57
AH-19[1]	10.04.02	8.8	3655	429	227	411	0.0006	0.1459	0.0166	1.4887	0.0180	61.24	4.51
AH-19[1]	23.07.02	6.8	3411	435	274	443	0.0005	0.0486	0.0163	1.6770	0.0192	58.56	4.15
AH-19[1]	14.11.02	9.2	3394	463	374	389	0.0004	0.0639	0.0120	1.3405	0.0123	60.73	5.58
AH-20[2]	10.04.02	6.5	3619	503	247	381	0.0004	0.1254	0.0104	1.1079	0.0157	91.83	3.84
AH-20[2]	24.07.02	6.4	3988	535	303	394	0.0004	0.1079	0.0174	1.3160	0.0165	94.93	3.94
AH-20[2]	13.11.02	6.3	3913	584	476	365	0.0004	0.1053	0.0088	0.9402	0.0130	93.34	2.26
AH-21[2]	09.04.02	6.9	4859	733	339	425	0.0007	0.1679	0.0150	1.6379	0.0337	138.97	5.30
AH-21[2]	24.07.02	6.4	5347	802	381	452	0.0005	0.0925	0.0118	1.3372	0.0266	140.12	5.97
AH-21[1]	21.11.02	6.4	5504	798	546	436	0.0005	0.0932	0.0106	1.4526	0.0262	143.37	4.69
AH-22[1]	10.04.02	6.4	2971	400	202	343	0.0011	0.1816	0.0296	2.5326	0.0359	124.07	4.17
AH-22[1]	23.07.02	6.8	3414	437	274	407	0.0009	0.1522	0.0221	2.2255	0.0317	121.04	4.51
AH-22[1]	14.11.02	7.4	3236	485	388	422	0.0009	0.1642	0.0245	2.5236	0.0291	122.52	3.40
AH-23[2]	10.04.02	6.5	3225	457	210	403	0.0050	0.3762	0.1170	8.3970	0.1512	344.04	6.03
AH-23[2]	09.08.02	6.2	3467	469	247	432	0.0041	0.2832	0.0576	6.6933	0.1205	341.57	8.00
AH-23[2]	14.11.02	6.6	3329	520	363	430	0.0034	0.2187	0.0374	6.0649	0.0912	379.12	5.58
AH-26[2]	09.04.02	7.0	3801	503	261	361	0.0017	0.4474	0.0247	3.2804	0.0740	263.98	6.63
AH-26[2]	23.07.02	6.4	4135	549	341	377	0.0016	0.2942	0.0259	3.3534	0.0692	278.73	7.08
AH-26[2]	14.11.02	6.4	3980	599	432	383	0.0015	0.2835	0.0210	3.4104	0.0624	282.99	6.28
AH-27[2]	10.04.02	6.7	4522	751	264	557	0.0016	0.2239	0.0232	2.9902	0.0919	250.06	6.84
AH-27[2]	25.07.02	6.2	5100	831	338	573	0.0017	0.2092	0.0282	3.6414	0.0879	235.44	6.80
AH-27[2]	13.11.02	6.4	4940	939	457	539	0.0019	0.2341	0.0214	3.2052	0.0828	248.05	4.51
AH-28[2]	24.07.02	6.4	4380	667	267	478	0.0001	0.0210	0.0086	0.7288	0.0048	57.69	3.82
AH-28[2]	13.11.02	6.5	4062	798	400	460	0.0002	0.0487	0.0069	0.7492	0.0062	64.57	3.41
AH-33B[2]	21.03.02	6.9	3802	568	250	477	0.0024	0.3465	0.0383	3.4364	0.0537	170.99	6.29
AH-33B[1]	08.04.02	7.1	2482	373	168	302	0.0024	0.2798	0.0351	3.9963	0.0545	204.17	9.71
AH-33B[2]	08.04.02	6.8	3846	575	250	481	0.0020	0.2383	0.0384	3.5462	0.0440	174.22	8.93
AH-33B[1]	23.04.02	7.3	3580	539	225	448	0.0015	0.1576	0.0197	3.2920	0.0341	209.87	6.48
AH-33B[1]	26.07.02	7.2	3988	598	238	442	0.0018	0.1741	0.0227	3.2421	0.0424	201.20	5.60
AH-33B[1]	05.09.02	7.6	3533	548	194	407	0.0015	0.1848	0.0202	3.4073	0.0307	189.22	7.95
AH-33B[2]	08.09.02	8.6	4040	611	215	460	0.0012	0.1378	0.0163	2.8111	0.0236	175.75	5.77
AH-33B[2]	02.10.02	6.9	4083	579	373	451	0.0016	0.1231	0.0203	3.3255	0.0293	178.84	5.62
AH-35A[1]	16.04.02	7.4	2189	246	85	436	0.0009	0.1520	0.0524	2.8201	0.0286	212.94	7.46
AH-35A[1]	05.06.02	7.5	1678	208	95	349	0.0007	0.0872	0.0170	2.0435	0.0189	201.76	9.31
AH-35A[1]	25.06.02	7.8	2028	239	81	358	0.0005	0.0463	0.0211	1.8324	0.0157	208.03	9.81
AH-35A[1]	21.11.02	7.6	2139	242	111	411	0.0004	0.0492	0.0140	1.6796	0.0140	204.75	9.13

1) Sample collected at wellhead with a webre separator;   2) Sample collected at wellhead separator.

TABLE 3:   The gas content of steam at 1 bar from Ahuachapán wells
(concentrations in mmoles/kg steam)

Well	Date of sampling	$P_{sampling}$ (bar-a)	He	H_2	Ar	N_2	CH_4	CO_2	H_2S	% CO_2	gases /steam (mg/kg)
AH-4BIS[2]	10.04.02	7.4	0	0.1067	0.0128	1.5308	0.0263	82.72	2.41	95	3,766
AH-4BIS[2]	25.07.02	6.8	0.0011	0.1211	0.0128	1.8060	0.0385	89.40	2.13	96	4,059
AH-4BIS[1]	13.11.02	7.0	0.0011	0.1174	0.0141	1.8307	0.0320	96.78	1.04	97	4,347
AH-6[2]	26.07.02	6.4	0.0006	0.2315	0.0115	1.3704	0.0289	147.05	5.30	95	6,692
AH-6[2]	12.11.02	6.4	0.0009	0.3274	0.0108	1.9576	0.0367	148.84	3.40	96	6,723
AH-16A[2]	09.04.02	7.2	0.0003	0.0734	0.0056	0.7485	0.0567	42.64	1.93	94	1,965
AH-16A[2]	12.11.02	6.6	0.0003	0.0629	0.0062	0.7250	0.0440	44.75	1.10	96	2,029
AH-17[2]	22.03.02	11.3	0.0007	0.0842	0.0077	1.5062	0.0201	110.35	4.43	95	5,050
AH-17[1]	25.07.02	11.8	0.0005	0.0462	0.0071	1.2381	0.0176	108.09	4.67	95	4,952
AH-17[1]	03.09.02	10.4	0.0005	0.0452	0.0047	1.0126	0.0140	111.04	4.52	95	5,070
AH-17[2]	15.11.02	11.8	0.0005	0.0513	0.0064	1.0665	0.0128	104.13	4.64	95	4,771
AH-17[1]	15.11.02	11.4	0.0005	0.0846	0.0081	1.3204	0.0127	116.88	3.77	96	5,310
AH-17[2]	15.11.02	7.0	0.0005	0.0575	0.0068	1.2003	0.0125	110.24	3.51	96	5,005
AH-19[1]	10.04.02	8.8	0.0001	0.0319	0.0036	0.3253	0.0039	13.38	0.99	91	632
AH-19[1]	23.07.02	6.8	0.0001	0.0132	0.0044	0.4555	0.0052	15.91	1.13	91	751
AH-19[1]	14.11.02	9.2	0.0001	0.0133	0.0025	0.2800	0.0026	12.69	1.17	90	606
AH-20[2]	10.04.02	6.5	0.0001	0.0398	0.0033	0.3517	0.0050	29.15	1.22	95	1,335
AH-20[2]	24.07.02	6.4	0.0001	0.0345	0.0056	0.4211	0.0053	30.38	1.26	95	1,392
AH-20[2]	13.11.02	6.3	0.0001	0.0340	0.0028	0.3033	0.0042	30.11	0.73	97	1,359
AH-21[2]	09.04.02	6.9	0.0002	0.0516	0.0046	0.5035	0.0103	42.72	1.63	95	1,950
AH-21[2]	24.07.02	6.4	0.0001	0.0296	0.0038	0.4279	0.0085	44.84	1.91	95	2,051
AH-21[1]	21.11.02	6.4	0.0002	0.0298	0.0034	0.4648	0.0084	45.88	1.50	96	2,084
AH-22[1]	10.04.02	6.4	0.0004	0.0660	0.0108	0.9202	0.0130	45.08	1.51	95	2,062
AH-22[1]	23.07.02	6.8	0.0003	0.0541	0.0078	0.7902	0.0113	42.98	1.60	95	1,969
AH-22[1]	14.11.02	7.4	0.0003	0.0564	0.0084	0.8664	0.0100	42.06	1.17	95	1,916
AH-23[2]	10.04.02	6.5	0.0020	0.1530	0.0476	3.4150	0.0615	139.92	2.45	96	6,340
AH-23[2]	09.08.02	6.2	0.0017	0.1165	0.0237	2.7543	0.0496	140.56	3.29	96	6,377
AH-23[2]	14.11.02	6.6	0.0014	0.0886	0.0152	2.4568	0.0369	153.58	2.26	97	6,906
AH-26[2]	09.04.02	7.0	0.0008	0.2010	0.0111	1.4739	0.0333	118.61	2.98	96	5,364
AH-26[2]	23.07.02	6.4	0.0007	0.1340	0.0118	1.5276	0.0315	126.97	3.23	96	5,742
AH-26[2]	14.11.02	6.4	0.0007	0.1291	0.0096	1.5536	0.0284	128.92	2.86	97	5,816
AH-27[2]	10.04.02	6.7	0.0006	0.0843	0.0087	1.1259	0.0346	94.16	2.58	96	4,264
AH-27[2]	25.07.02	6.2	0.0007	0.0807	0.0109	1.4054	0.0339	90.87	2.62	96	4,129
AH-27[2]	13.11.02	6.4	0.0007	0.0895	0.0082	1.2247	0.0316	94.78	1.72	97	4,265
AH-28[2]	24.07.02	6.4	0.0000	0.0065	0.0026	0.2244	0.0015	17.76	1.18	93	828
AH-28[2]	13.11.02	6.5	0.0001	0.0149	0.0021	0.2287	0.0019	19.71	1.04	94	909
AH-33B[2]	21.03.02	6.9	0.0008	0.1147	0.0127	1.1376	0.0178	56.60	2.08	94	2,595
AH-33B[1]	08.04.02	7.1	0.0008	0.0914	0.0115	1.3050	0.0178	66.67	3.17	94	3,080
AH-33B[2]	08.04.02	6.8	0.0007	0.0794	0.0128	1.1817	0.0146	58.05	2.98	93	2,690
AH-33B[1]	23.04.02	7.3	0.0005	0.0508	0.0064	1.0608	0.0110	67.63	2.09	95	3,078
AH-33B[1]	26.07.02	7.2	0.0006	0.0565	0.0074	1.0519	0.0137	65.28	1.82	96	2,965
AH-33B[1]	05.09.02	7.6	0.0005	0.0584	0.0064	1.0763	0.0097	59.77	2.51	94	2,747
AH-33B[2]	08.09.02	8.6	0.0004	0.0408	0.0048	0.8315	0.0070	51.98	1.71	95	2,370
AH-33B[2]	02.10.02	6.9	0.0005	0.0408	0.0067	1.1008	0.0097	59.20	1.86	95	2,700
AH-35A[1]	16.04.02	7.4	0.0003	0.0505	0.0174	0.9366	0.0095	70.72	2.48	95	3,224
AH-35A[1]	05.06.02	7.5	0.0002	0.0267	0.0052	0.6264	0.0058	61.84	2.85	95	2,837
AH-35A[1]	25.06.02	7.8	0.0001	0.0139	0.0063	0.5497	0.0047	62.41	2.94	95	2,863
AH-35A[1]	21.11.02	7.6	0.0001	0.0150	0.0043	0.5111	0.0043	62.30	2.78	95	2,851

1) Sample collected at wellhead with a webre separator;   2) sample collected at wellhead separator.

TABLE 4: The gas content of steam at 1 bar from Berlín wells[1]
(concentrations in mmoles/kg steam)

Well	Date of sampling	$P_{sampling}$ (bar-a)	He	H_2	Ar	N_2	CH_4	CO_2	H_2S	% CO_2	gases /steam (mg/kg)
TR-2	13.04.02	12.7	0.0002	0.0863	0.0076	0.5670	0.0115	30.46	5.78	83	1554
TR-2	19.06.02	13.2	0.0001	0.0609	0.0113	0.5747	0.0149	29.09	6.94	79	1534
TR-2	27.09.02	11.6	0.0001	0.0709	0.0069	0.5580	0.0095	28.30	7.15	78	1,505
TR-4B	19.06.02	14.0	0.0002	0.3044	0.0311	1.3827	0.0422	66.12	7.78	87	3,216
TR-4B	19.09.02	15.0	0.0002	0.3517	0.0116	1.1339	0.0168	60.93	7.43	87	2,968
TR-4C	26.04.02	11.5	0.0003	0.4071	0.0203	1.3279	0.0295	48.31	5.52	87	2,354
TR-4C	19.06.02	12.5	0.0002	0.5966	0.0228	0.9493	0.0212	45.73	7.38	84	2,293
TR-4C	19.09.02	11.7	0.0002	0.2832	0.0158	0.9914	0.0203	46.24	8.71	82	2,361
TR-5A	18.06.02	12.0	0.0003	0.1046	0.0045	0.9485	0.0183	27.90	7.02	77	1,495
TR-5A	00.01.00	14.5	0.0002	0.0662	0.0075	0.6700	0.0080	24.19	5.65	79	1277
TR-5B	18.06.02	12.6	0.0003	0.1388	0.0092	0.7746	0.0085	27.78	6.35	79	1462
TR-5B	18.09.02	14.2	0.0002	0.0746	0.0087	0.7070	0.0104	33.316	5.52	84	1675
TR-5C	25.04.02	13.5	0.0002	0.0845	0.0043	0.5240	0.0088	28.99	6.34	81	1507
TR-5C	18.06.02	13.6	0.0001	0.0435	0.0050	0.4014	0.0116	30.88	6.09	82	1578
TR-5V	24.04.02	11.1	0.0003	0.0976	0.0077	0.7977	0.0140	36.78	8.21	80	1922
TR-5V	13.06.02	12.9	0.0002	0.0719	0.0146	0.8012	0.0194	35.47	6.46	83	1805
TR-5V	18.09.02	11.0	0.0003	0.1082	0.0091	0.8572	0.0134	36.06	7.01	82	1851
TR-9	13.04.02	18.2	0.0001	0.0870	0.0032	0.5542	0.0071	33.27	4.87	86	1646
TR-9	20.06.02	11.4	0.0001	0.0690	0.01	0.3899	0.01	28.93	6	82	1487
TR-9	26.09.02	11.8	0	0.1111	0.0052	0.3967	0.01	30.51	5.88	83	1555

1) Samples collected at wellhead with a webre separator.